

Memory Effects in Quantum State Verification

Siyuan Chen,^{1,2} Wei Xie,³ and Kun Wang^{1,*}

¹*Institute for Quantum Computing, Baidu Research, Beijing 100193, China*

²*Physics Department, Jilin University*

³*School of Computer Science and Technology, University of Science and Technology of China*

(Dated: April 9, 2024)

We consider the quantum memory assisted state verification task, where the local verifiers can store copies of quantum states and measure them collectively. We establish an exact analytic formula for optimizing two-copy state verification and give a globally optimal two-copy strategy for multi-qubit graph states involving only Bell measurements. When arbitrary memory is available to the verifiers, we present a dimension expansion technique that designs efficient verification strategies, showcasing its application to GHZ-like states. These strategies become increasingly advantageous with growing memory resources, ultimately approaching the theoretical limit of efficiency. Our findings demonstrate that quantum memories enhance state verification efficiency, shedding light on error-resistant strategies and practical applications of large-scale quantum memory-assisted verification.

Introduction.—The precise and efficient characterization of quantum states is a pivotal endeavor in many quantum information processing tasks such as quantum teleportation [1], quantum cryptography [2], and measurement-based quantum computation [3]. While the tomography method theoretically possesses the capability to reconstruct the complete density matrix [4], its computational demands and time-consuming nature become particularly pronounced as the size of the quantum system increases, due to the curse of dimensionality. Fortunately, the need for tomography diminishes when our focus is narrowed to specific characteristics of quantum systems. Numerous statistical methods have been devised for quantum certification, validation, and benchmarking [5, 6]. Among these, quantum state verification (QSV) [7–16] not only accurately estimates the quality of the quantum states but also consumes an exponentially smaller number of quantum state copies, thus emerging as a highly potential tool. We refer the interested readers to [17] and references therein.

In QSV, we consider a quantum device designed to produce a multipartite pure state $|\psi\rangle$. Throughout this work, we assume that $|\psi\rangle$ is n -partite and each party is d -dimensional, with associated Hilbert space \mathcal{H} . However, it might work incorrectly and outputs independent states $\sigma_1, \sigma_2, \dots, \sigma_N$ in N runs. It is guaranteed that either $\sigma_j = |\psi\rangle\langle\psi|$ for all j (good case) or $\langle\psi|\sigma_j|\psi\rangle \leq 1 - \varepsilon$ for all j (bad case). After receiving these states, a verifier performs two-outcome measurements randomly chosen from a set of available measurements. Each two-outcome measurement $\{T_\ell, \mathbb{1} - T_\ell\}$ is specified by some operator T_ℓ and is performed with probability p_ℓ , corresponding to passing the test. In the bad case, the maximal probability that σ_j passes the test satisfies [8]

$$\max_{\langle\psi|\sigma_j|\psi\rangle \leq 1 - \varepsilon} \text{Tr}[\Omega\sigma_j] = 1 - (1 - \lambda_2(\Omega))\varepsilon, \quad (1)$$

where $\Omega = \sum_\ell p_\ell T_\ell$ is a verification strategy and $\lambda_2(\Omega)$ is the second largest eigenvalue of Ω . In the bad case, all the N sampled quantum states can pass the test with probability

at most $[1 - (1 - \lambda_2(\Omega))\varepsilon]^N$. Hence to achieve certain fixed worst-case failure probability δ , it suffices to take

$$N(\Omega) = \frac{\ln \delta}{\ln[1 - (1 - \lambda_2(\Omega))\varepsilon]} \approx \frac{1}{(1 - \lambda_2(\Omega))\varepsilon} \ln \frac{1}{\delta}, \quad (2)$$

where \ln denotes the natural logarithm and the approximation holds when ε is small. We call $N(\Omega)$ the sample complexity of the verification strategy Ω in abuse of notation. Specially, the globally optimal strategy $\{|\psi\rangle\langle\psi|, \mathbb{1} - |\psi\rangle\langle\psi|\}$ has sample complexity $N_{\text{glob}} \approx 1/\varepsilon \ln 1/\delta$. We say a strategy achieves globally optimal efficiency if its sample complexity scales as N_{glob} . While the globally optimal strategy offers exceptional efficiency, its reliance on entangled measurements poses challenges in experimental implementation. Thus, we focus on designing efficient strategies that leverage only local measurements and classical communication, making them amenable to practical applications.

Motivation.—Quantum memories, analogous to the digital memory used in classical computers, have been realized in diverse physical systems [18]. For example, Bhaskar *et al.* [19] demonstrated an integrated single solid-state spin memory for implementing asynchronous photonic Bell-state measurements, a crucial element in quantum repeaters. Advances in quantum memories offer substantial benefits to burgeoning quantum technologies such as quantum key distribution [19] and quantum control [20], and fundamentally revolutionize our understanding of physical phenomena like the uncertainty principle [21]. Given these promising developments, the question naturally arises: Can we harness quantum memories to enhance quantum state verification?

Two preceding studies have demonstrated the potential of quantum memory to improve the efficiency of quantum state verification, albeit from different viewpoints. Liu *et al.* [13] constructed a universally optimal protocol for verifying entangled states by employing quantum nondemolition measurements. This protocol's practicality is limited by the entangled operations between memory qubits and all parties. Miguel-Ramiro *et al.* [14] introduced collective strategies for the efficient, local verification of ensembles of Bell pairs. However, their strategies are limited to Bell states and GHZ states with Werner-type noise and require error number gates (ENG).

* nju.wangkun@gmail.com

In this Letter, we delineate the intrinsic value $\lambda_*(\Omega)$ for any two-copy verification strategy Ω that underpins its verification efficiency. Furthermore, we propose a dimension expansion method for constructing copies greater than two. This takes a crucial step in this direction, demonstrating how to construct the most efficient QSV strategy under constraints of limited quantum memories.

Quantum memory assisted state verification.—In this verification strategy, n spatially disparate verifiers conduct a test as follows: First, they store k copies of d -dimensional qudits in their local quantum memories; Then, they measure their local copies in $\mathcal{H}^k \equiv \mathcal{H}^{\otimes k}$ using (possibly entangled) measurements and make a decision based on the outcomes. This “store-and-measure” strategy is vividly illustrated in Fig. 1 for $k = 2$. The test will be repeated M times and the total number of consumed states is Mk . We designate this quantum memory-assisted strategy as an (n, k, d) verification strategy. Its crucial distinction from standard verification strategies, comprehensively reviewed in [17], lies in the latter’s absence of quantum memory assistance. In our notation, these standard strategies fall under the category of $(n, 1, d)$ strategies. In the good case, the overall state stored in the quantum memories admits a tensor product structure: $|\Psi\rangle := \bigotimes_{r=1}^k |\psi\rangle^{(r)}$, where the superscript r represents the r -th copy in the quantum memory. The verifiers perform a local binary measurement $\{T_\ell, \mathbb{1} - T_\ell\}$ such that state $|\Psi\rangle$ passes the test with certainty. In the bad case, we assume that the k states produced by the quantum device are independent, indicating that the fake state in the composite space \mathcal{H}^{nk} has the form

$$\xi = \bigotimes_{r=1}^k \sigma^{(r)}, \quad (3)$$

where each $\sigma^{(r)}$ satisfies $\langle \psi | \sigma^{(r)} | \psi \rangle \leq 1 - \varepsilon$. Correspondingly, the maximal probability that the fake state ξ in the bad case can pass the test is

$$p(\Omega) := \max_{\langle \psi | \sigma^{(r)} | \psi \rangle \leq 1 - \varepsilon} \text{Tr} \left[\Omega \left(\bigotimes_{r=1}^k \sigma^{(r)} \right) \right]. \quad (4)$$

The minimum required number of measurements to saturate the worst-case failure probability, denoted as $M_m(\Omega)$, is given by $M_m(\Omega) = \ln \delta / \ln p(\Omega)$. Thus, the total number of copies consumed by the verification strategy Ω satisfies

$$N_m(\Omega) = k M_m(\Omega) = \frac{k \ln \delta}{\ln p(\Omega)}. \quad (5)$$

The verifiers’ objective is to design efficient memory-assisted strategies Ω that minimize the number of copies consumed.

Two-copy verification strategy.—We analytically solve the maximization problem in Eq. (4) for the case of $k = 2$, yielding an exact analytic formula for optimizing two-copy state verification. First of all, we simplify the form of the optimization in Eq. (4). Regarding the permutation invariant nature of the verifiers, we show that it is best to consider verification strategies that are symmetric with respect to the two state copies; i.e., $\mathbb{F}_{1 \leftrightarrow 2} \Omega \mathbb{F}_{1 \leftrightarrow 2} = \Omega$, where $\mathbb{F}_{1 \leftrightarrow 2}$ is the swap operator between the first and second copy. Regarding Eq. (4), we

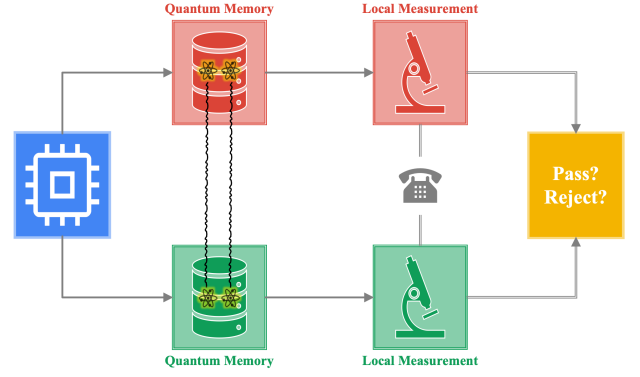


FIG. 1. Schematic view of quantum memory assisted state verification. In this $(2, 2, d)$ strategy, the verifiers store two copies of quantum states (represented by atoms) in their local quantum memories. They then agree on local measurements via classical communication and perform these measurements on their respective qudits. Finally, they make a “pass/reject” decision from the measurement outcomes.

make the following useful observations: (a) It suffices to optimize over pure fake states; and (b) If the quantum device is not too bad, i.e., there exists an *insurance infidelity* $\varepsilon_{\max} \geq \varepsilon$ such that $\langle \psi | \sigma | \psi \rangle \geq 1 - \varepsilon_{\max}$ for all σ , it is then suffices to consider fake states σ for which $\langle \psi | \sigma | \psi \rangle = 1 - \varepsilon$. We prove these observations in Appendix A, where we elaborate the significance and bounds of the insurance infidelity parameter ε_{\max} . We introduce the following two projectors:

$$\mathbb{P}_s := \frac{\mathbb{F}_{1 \leftrightarrow 2} + \mathbb{I}_{12}}{2}, \quad \mathbb{P}_\psi := |\psi\rangle\langle\psi| \otimes (\mathbb{I} - |\psi\rangle\langle\psi|), \quad (6)$$

which are useful in deriving the analytic formula. Note that \mathbb{P}_s is the projector onto the symmetric subspace of $\mathcal{H}^n \otimes \mathcal{H}^n$. For any symmetric two-copy verification strategy Ω , define the doubly projected operator $\Omega_\star := 2\mathbb{P}_\psi \mathbb{P}_s \Omega \mathbb{P}_s \mathbb{P}_\psi$. Let $\lambda_*(\Omega)$ be the maximal eigenvalue of the projected operator Ω_\star . We show that, λ_* is the intrinsic property of Ω which underpins Ω ’s verification efficiency, as elucidated in the ensuing theorem. The proof can be found in Appendix A.

Theorem 1. *When $\lambda_*(\Omega) < 1$ and the existence of insurance fidelity ε_{\max} is guaranteed, it holds that*

$$p(\Omega) = 1 - 2(1 - \lambda_*(\Omega))\varepsilon + \mathcal{O}(\varepsilon^{1.5}). \quad (7)$$

Correspondingly, the sample complexity of Ω is given by

$$N_m(\Omega) = \frac{2 \ln \delta}{\ln p(\Omega)} \approx \frac{1}{(1 - \lambda_*(\Omega))\varepsilon} \ln \frac{1}{\delta}. \quad (8)$$

Comparing Eqs. (2) and (8), we see that it is $\lambda_*(\Omega)$, instead of $\lambda_2(\Omega)$, that determines the sample complexity of Ω in the memory assisted scenario. For the tensor product of single-copy globally optimal strategies, $\Omega_g = |\psi\rangle\langle\psi|^{\otimes 2}$, we find that $\lambda_*(\Omega_g) = 0$, implying a sample complexity of $1/\varepsilon \ln 1/\delta$. This confirms that, in this specific case, quantum memory assistance cannot surpass the ultimate bound established by entangled measurements. Similarly, for a tensor product strategy

$\Omega = \Omega_l \otimes \Omega_l$, where Ω_l is any single-copy local verification strategy and quantum memories are absent, $\lambda_*(\Omega) = \lambda_2(\Omega_l)$, reducing precisely to the single-copy case. These examples demonstrate the alignment of our findings with existing results. Extending Theorem 1 for arbitrary k is possible through generalized versions of \mathbb{P}_s and \mathbb{P}_ψ . However, two-copy verification strategies already showcase the potential to achieve globally optimal efficiency as we will show in the following examples. Moreover, the fidelity and coherence time requirements of quantum memory devices become increasingly stringent with larger k , potentially hindering their feasibility for practical applications beyond a certain threshold.

Graph states. As paradigmatic examples of quantum states which exhibit genuine multipartite entanglement, graph states hold central importance in quantum computation and information due to their unique entanglement structure [22–25]. A graph state is associated with a graph $G = (V, E)$. It can be prepared through Hadamard gates on qubit vertices in V followed by control-Z gates on edges in E . A simple example of graph state is G_0 : $\bullet\text{---}\bullet\text{---}\bullet$, whose corresponding graph state is:

$$|G_0\rangle = \frac{1}{\sqrt{8}}(|000\rangle + |100\rangle + |010\rangle - |110\rangle + |001\rangle + |101\rangle - |011\rangle + |111\rangle). \quad (9)$$

We leverage Theorem 1 to construct a two-copy verification strategy for arbitrary multi-qubit graph state $|G\rangle$, demonstrating that even moderate quantum memory usage can boost the QSV efficiency to global optimality.

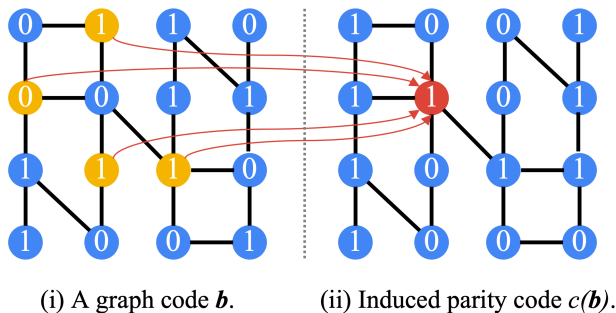


FIG. 2. Schematic view of a graph code \mathbf{b} of a graph and its induced parity code $\mathbf{c}(\mathbf{b})$. The binary value of a vertex (red vertex) in the induced parity code is given by the summation modulus 2 of the values of its adjacent vertices (yellow vertices) in the graph code \mathbf{b} .

To formally describe our two-copy verification strategy for graph states, we begin by introducing the concept of graph code of a graph $G = (V, E)$. Let $n = |V|$ be the number of vertices. A *graph code* $\mathbf{b} \in \{0, 1\}^n$ is an n -bit binary string that assigns the binary value $\mathbf{b}_v \in \{0, 1\}$ to vertex $v \in V$. Fig. 2(i) visualizes a graph code of G for example. Each graph code \mathbf{b} uniquely induces a *parity code* $\mathbf{c}(\mathbf{b}) \in \{0, 1\}^n$, where the binary string map $c : \{0, 1\}^n \rightarrow \{0, 1\}^n$ is defined as $c_u(\mathbf{b}) := \sum_{v \in V, u \sim v} \mathbf{b}_v \pmod{2}$, c_u is the value of vertex u , and $u \sim v$ means that u is adjacent to v . An illustrative example is presented in Fig. 2(ii). Let $|\Phi_{00}\rangle := (|00\rangle + |11\rangle)/\sqrt{2}$

be the standard two-qubit Bell state. A binary code pair (z, x) induces a locally transformed Bell state via

$$|\Phi_{zx}\rangle := (\mathbb{I} \otimes X^x Z^z)|\Phi_{00}\rangle, \quad (10)$$

where X and Z are the Pauli operators. Our two-copy strategy for $|G\rangle$ involves only one binary measurement $\{\Omega_g, \mathbb{I} - \Omega_g\}$, where Ω_g corresponding to passing the test is defined as

$$\Omega_g = \sum_{\mathbf{b} \in \{0, 1\}^n} \bigotimes_{j=1}^n |\Phi_{c_j(\mathbf{b})\mathbf{b}_j}\rangle \langle \Phi_{c_j(\mathbf{b})\mathbf{b}_j}|_{O_j O'_j}, \quad (11)$$

where O_j, O'_j represent two qubits held by the j -th verifier. The verification strategy carries out as follows. In each test, the verifiers first store two copies of the states. Then, the j -th verifier measures his qubits $O_j O'_j$ with the Bell measurement $\{|\Phi_{zx}\rangle \langle \Phi_{zx}|\}_{x,z \in \{0,1\}}$ and records the outcome as $\mathbf{b}_j = x$ and $\mathbf{b}'_j = z$. Finally, they classically communicate the outcomes and obtain two graph codes \mathbf{b}, \mathbf{b}' of the graph G . The states pass the test if and only if $\mathbf{b} = \mathbf{c}(\mathbf{b}')$.

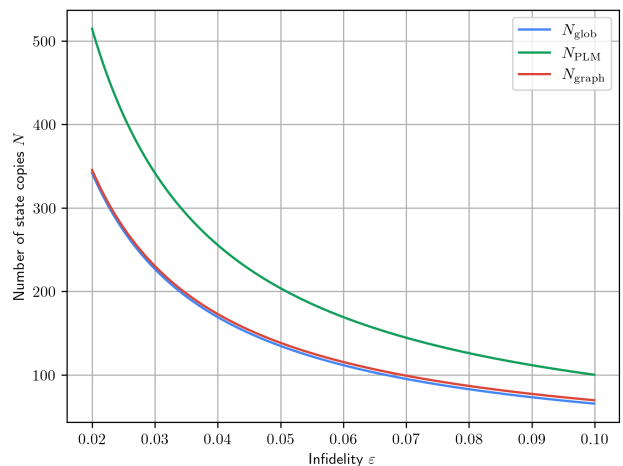


FIG. 3. Comparison of the total number of state copies required to verify the Bell state for different strategies as a function of the infidelity ϵ , where $\delta = 0.001$. Here, N_{graph} is the sample complexity of our proposed two-copy graph verification strategy, N_{PLM} is the sample complexity of the optimal strategy by Pallister *et al.* [8], and N_{glob} is the sample complexity of the globally optimal strategy.

Regarding the performance of our two-copy verification strategy Ω_g , we prove in Appendix D that $\lambda_*(\Omega_g) = 0$ and thus its optimal efficiency is achieved with a sample complexity of $N_{\text{graph}}(\Omega_g) \approx 1/\epsilon \ln 1/\delta$ using Eq. (8), indicating that Ω_g achieves globally optimal efficiency. To showcase its significant advantage, we compare its efficiency with the optimal single-copy verification strategy by Pallister *et al.* [8] on verifying the canonical Bell state $|\Phi_{00}\rangle$. As shown in Fig. 3, our two-copy strategy rapidly converges towards the globally optimal solution in the small ϵ regime, reducing the sample complexity by 50% compared to the optimal single-copy verification strategy. This demonstrates a remarkable improvement in verification efficiency assisted by quantum memory. Note that our two-copy verification strategy for the Bell state bears

similarities with the celebrated entanglement-swapping protocol [26, 27], an important component of quantum networks.

Several remarks are in order. First, the construction of the above two-copy verification strategy for graph states, whose details can be found in Appendices B, C, and D, is conceptually insightful and potentially extensible. Briefly, we begin by establishing an equivalence between information-preserving channels and optimal strategies, converting the verification problem to a state discrimination problem. Subsequently, we demonstrate that graph states can be leveraged to locally implement control- Z gates, capitalizing on their inherent entanglement structure. This allows us to construct a quantum channel which induces the aforementioned strategy. Second, the consistent Bell measurement across different verifiers, a key feature of our two-copy strategy, offers significant advantages for conducting state verification in neutral atom-based quantum systems [28]. This consistency simplifies the verification process as a global laser can be employed, leveraging the Rydberg blockade radius, to parallelly execute Bell measurements on all qubit pairs without single addressing [29]. Third, we illustrate in Appendix E that, the verification strategy can be adapted to accomplish fidelity estimation. Let σ and σ' be the unknown states produced in two device calls. If the target quantum device is guaranteed to produce independent states, it holds that

$$p_s = \text{Tr}[\Omega_g(\sigma \otimes \sigma')] = \langle G|\sigma|G\rangle\langle G|\sigma'|G\rangle + \mathcal{O}(\varepsilon^2). \quad (12)$$

Thus, when ε is sufficiently small, the average fidelity \mathcal{F} of the states σ with the target state $|G\rangle$ can be estimated from the statistical average of the passing frequency p_s via $\mathcal{F} = \sqrt{p_s}$.

Dimension expansion.—In the two-copy verification, we analytically solved the maximization problem in Eq. (4), relating the verification efficiency to an intrinsic property of Ω . However, it is demanding to generalize the result to larger k . Inspired by the observation that every k -tensor state $|\Psi\rangle$ can be equivalently viewed as a single n -partite state with local dimension d^k , we present the dimension expansion method that construct (n, k, d) -QSV protocol according to existing $(n, 1, d^k)$ -QSV protocol with unchanged efficiency. This “dimension expansion” from d to d^k leverages quantum memory and establish an equivalence between an $(n, 1, d^k)$ verification strategy and an (n, k, d) strategy. Concretely, we relax the maximization problem in Eq. (4) by considering any quantum state ξ in \mathcal{H}^{n^k} satisfying the fidelity constraint $\langle \Psi|\xi|\Psi\rangle \leq (1 - \varepsilon)^k$, providing an upper bound for the worst-case passing probability $p(\Omega)$:

$$p(\Omega) \leq \max_{\langle \Psi|\xi|\Psi\rangle \leq (1-\varepsilon)^k} \text{Tr}[\Omega\xi] = 1 - (1 - \lambda_2(\Omega))\varepsilon', \quad (13)$$

where $\varepsilon' := 1 - (1 - \varepsilon)^k$ and the equality follows from Eq. (1). Correspondingly, we obtain an upper bound on $N_m(\Omega)$:

$$N_m(\Omega) \leq \frac{1}{(1 - \lambda_2(\Omega))\varepsilon} \ln \frac{1}{\delta} =: N_{\text{de},k}(\Omega). \quad (14)$$

Interestingly, $N_{\text{de},k}(\Omega)$ is completely determined by $\lambda_2(\Omega)$, analogous to the single-copy state verification case.

When investigating quantum memory assisted state verification, we have imposed two critical properties: (i) Locality:

the fake states generated by the quantum device are independent; and (ii) Trust: the quantum memories are faithful without experimental error. If either property is violated, the k -copy fake state might possess quantum correlation, leading to $N_m = N_{\text{de},k}$ as evident from Eqs. (13) and (14). This signifies $N_{\text{de},k}$ as a fundamental upper bound on the efficiency of quantum memory assisted state verification.

GHZ-like states. We demonstrate the power of the dimension expansion technique in constructing verification strategies for a broad class of GHZ-like states, encompassing arbitrary bipartite qudit states and GHZ states as special cases. Mathematically, a multi-qudit GHZ-like state is defined as

$$|\psi_{\text{GHZ}}\rangle := \sum_{j=0}^{d-1} s_j |j_1\rangle \otimes \cdots \otimes |j_n\rangle, \quad (15)$$

where $\{|j_r\rangle\}_j$ is an orthonormal basis of the r -th qudit, and the non-negative coefficients s_j are decreasingly sorted and satisfy $\sum_j s_j^2 = 1$. Whenever $s_0 < 1$, the GHZ state is entangled. Note that the k -th tensor of a GHZ-like state is still a GHZ-like state, but with different coefficients.

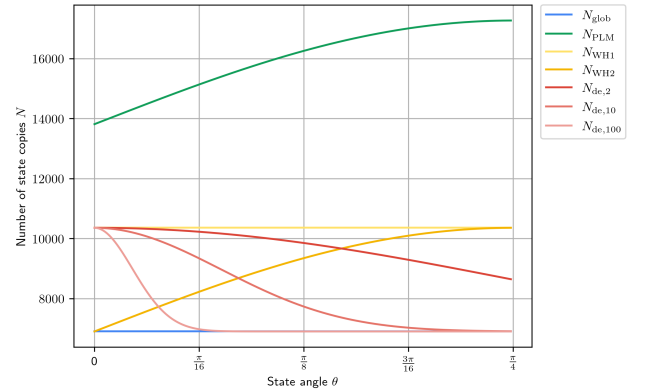


FIG. 4. Comparison of the total number of state copies required to verify the bipartite pure state $|\psi\rangle = \cos\theta|00\rangle + \sin\theta|11\rangle$ for different strategies, where $\varepsilon = \delta = 0.001$. Here, $N_{\text{de},k}$ is the sample complexity of our proposed dimension expansion strategy, N_{PLM} is the sample complexity of the optimal local strategy by Pallister *et al.* [8], N_{WH1} and N_{WH2} are the sample complexities of the optimal one-way and two-way LOCC strategies by Wang and Hayashi [10], and N_{glob} is the sample complexity of the globally optimal strategy.

Li *et al.* [30] designed an efficient $(n, 1, d)$ verification strategy Ω_{LHZ} for GHZ-like states satisfying $\lambda_2(\Omega_{\text{LHZ}}) = ((n-1)s_0^2 + s_1^2)/(n + (n-1)s_0^2 + s_1^2)$. The (n, k, d) -dimension expansion strategy for $|\psi_{\text{GHZ}}\rangle$, which is deduced from the $(n, 1, d^k)$ strategy for the k -th tensor product state $|\psi_{\text{GHZ}}\rangle^{\otimes k}$, has the sample complexity

$$N_{\text{de},k}(|\psi_{\text{GHZ}}\rangle) = \frac{n + (n-1)s_0^{2k} + s_0^{2k-2}s_1^2}{n\varepsilon} \ln \frac{1}{\delta}. \quad (16)$$

One can verify that $N_{\text{de},k}$ is monotonically decreasing in k ; i.e., $k \geq k'$ implies $N_{\text{de},k}(|\psi_{\text{GHZ}}\rangle) \leq N_{\text{de},k'}(|\psi_{\text{GHZ}}\rangle)$. Whenever $s_0 < 1$, indicating that the state is entangled, the dimension expansion strategy consistently outperforms the standard strategy with a *net* benefit ratio of s_0^{2k-2} and approaches

the globally optimal efficiency when k is sufficiently large. Practically, the integer k is upper bounded by $N_{de,k}$.

In Figure 4, the sample complexity required to verify the two-qubit state $|\psi_\theta\rangle = \cos\theta|00\rangle + \sin\theta|11\rangle$, being a special case of the GHZ-like states, is shown for different verification strategies. We give the explicit construction of its verification strategy in Appendix F. The dimension expansion strategy derived here gives a remarkable improvement over the previously optimal local strategy by Pallister *et al.* [8] and optimal one-way LOCC strategy by Wang and Hayashi [10] for the full range of $\theta \in (0, \pi/4)$, for the given values ε and δ . Furthermore, it is evident from the figure that the dimension expansion strategy becomes more and more advantageous as k increases, eventually exceeding the optimal two-way LOCC strategy [10] and approaching the globally optimal efficiency, revealing the power of dimension expansion strategy.

Conclusions.—We have proposed a theoretical framework to quantitatively analyze the performance boost offered by

quantum memories in quantum state verification. Our work demonstrates that memory-assisted verification strategies significantly outperform non-assisted ones, with a remarkable finding that even just two copies suffice to achieve the theoretical limit of verification efficiency. This superiority lies in the extended storage capacity, enabling the verifier to perform powerful entangled measurements within the memory.

Many questions remain open. Specifically, the analytic formula for two-copy verification and the optimal two-copy strategy for graph states might be generalized to wider scenarios with larger amount of quantum memories and arbitrary quantum states. However, deriving such solutions will likely require innovative techniques due to increased computational demands and higher state dimensions.

Acknowledgements.—We thank Tianchen Qu and Kun Fang for their insightful discussions. This work was done when S. C. was a research intern at Baidu Research.

-
- [1] C. H. Bennett, G. Brassard, C. Crépeau, R. Jozsa, A. Peres, and W. K. Wootters, *Physical Review Letters* **70**, 1895 (1993).
- [2] S. Pirandola, U. L. Andersen, L. Banchi, M. Berta, D. Bunandar, R. Colbeck, D. Englund, T. Gehring, C. Lupo, C. Ottaviani, *et al.*, *Advances in Optics and Photonics* **12**, 1012 (2020).
- [3] D. Gottesman and I. L. Chuang, *Nature* **402**, 390 (1999).
- [4] G. M. D’Ariano, M. De Laurentis, M. G. Paris, A. Porzio, and S. Solimeno, *Journal of Optics B: Quantum and Semiclassical Optics* **4**, S127 (2002).
- [5] J. Eisert, D. Hangleiter, N. Walk, I. Roth, D. Markham, R. Parekh, U. Chabaud, and E. Kashefi, *Nature Reviews Physics* **2**, 382 (2020).
- [6] M. Kliesch and I. Roth, *PRX Quantum* **2**, 010201 (2021).
- [7] M. Hayashi and T. Morimae, *Physical Review Letters* **115**, 220502 (2015).
- [8] S. Pallister, N. Linden, and A. Montanaro, *Physical Review Letters* **120**, 170502 (2018).
- [9] H. Zhu and M. Hayashi, *Physical Review Letters* **123**, 260504 (2019).
- [10] K. Wang and M. Hayashi, *Physical Review A* **100**, 032315 (2019).
- [11] Z. Li, Y.-G. Han, and H. Zhu, *Physical Review A* **100**, 032316 (2019).
- [12] X.-D. Yu, J. Shang, and O. Gühne, *npj Quantum Information* **5**, 10.1038/s41534-019-0226-z (2019).
- [13] Y.-C. Liu, J. Shang, R. Han, and X. Zhang, *Physical Review Letters* **126**, 090504 (2021).
- [14] J. Miguel-Ramiro, F. Riera-Sàbat, and W. Dür, *Physical Review Letters* **129**, 190504 (2022).
- [15] W.-H. Zhang, C. Zhang, Z. Chen, X.-X. Peng, X.-Y. Xu, P. Yin, S. Yu, X.-J. Ye, Y.-J. Han, J.-S. Xu, G. Chen, C.-F. Li, and G.-C. Guo, *Physical Review Letters* **125**, 030506 (2020).
- [16] X. Jiang, K. Wang, K. Qian, Z. Chen, Z. Chen, L. Lu, L. Xia, F. Song, S. Zhu, and X. Ma, *npj Quantum Information* **6**, 10.1038/s41534-020-00317-7 (2020).
- [17] X.-D. Yu, J. Shang, and O. Gühne, *Advanced Quantum Technologies* **5**, 2100126 (2022).
- [18] K. Heshami, D. G. England, P. C. Humphreys, P. J. Bustard, V. M. Acosta, J. Nunn, and B. J. Sussman, *Journal of Modern Optics* **63**, 2005 (2016).
- [19] M. K. Bhaskar, R. Riedinger, B. Machielse, D. S. Levonian, C. T. Nguyen, E. N. Knall, H. Park, D. Englund, M. Lončar, D. D. Sukachev, *et al.*, *Nature* **580**, 60 (2020).
- [20] M. Roget, B. Herzog, and G. Di Molfetta, *Scientific Reports* **10**, 21354 (2020).
- [21] P. J. Coles, M. Berta, M. Tomamichel, and S. Wehner, *Rev. Mod. Phys.* **89**, 015002 (2017).
- [22] R. Raussendorf and H. J. Briegel, *Phys. Rev. Lett.* **86**, 5188 (2001).
- [23] O. Gühne, G. Tóth, P. Hyllus, and H. J. Briegel, *Phys. Rev. Lett.* **95**, 120405 (2005).
- [24] A. Broadbent, J. Fitzsimons, and E. Kashefi, in *2009 50th Annual IEEE Symposium on Foundations of Computer Science (IEEE, 2009)*.
- [25] S. Perseguers, G. J. Lapeyre, D. Cavalcanti, M. Lewenstein, and A. Acín, *Reports on Progress in Physics* **76**, 096001 (2013).
- [26] M. Żukowski, A. Zeilinger, M. A. Horne, and A. K. Ekert, *Phys. Rev. Lett.* **71**, 4287 (1993).
- [27] M. Halder, A. Beveratos, N. Gisin, V. Scarani, C. Simon, and H. Zbinden, *Nature Physics* **3**, 692–695 (2007).
- [28] D. Bluvstein, S. J. Evered, A. A. Geim, S. H. Li, H. Zhou, T. Manovitz, S. Ebadi, M. Cain, M. Kalinowski, D. Hangleiter, J. P. B. Ataiades, N. Maskara, I. Cong, X. Gao, P. S. Rodriguez, T. Karolyshyn, G. Semeghini, M. J. Gullans, M. Greiner, V. Vuletić, and M. D. Lukin, *Nature* **10.1038/s41586-023-06927-3** (2023).
- [29] Y. Wang, A. Kumar, T.-Y. Wu, and D. S. Weiss, *Science* **352**, 1562 (2016).
- [30] Z. Li, Y.-G. Han, and H. Zhu, *Physical Review Applied* **13**, 054002 (2020).
- [31] S. Pallister, *PhD thesis, University of Bristol* (2018).
- [32] E. Chitambar, D. Leung, L. Mančinska, M. Ozols, and A. Winter, *Communications in Mathematical Physics* **328**, 303 (2014).
- [33] J. Eisert, K. Jacobs, P. Papadopoulos, and M. B. Plenio, *Physical Review A* **62**, 052317 (2000).
- [34] A. M. Steane, *Nature* **399**, 124 (1999).
- [35] M. Van den Nest, J. Dehaene, and B. De Moor, *Phys. Rev. A* **69**, 022316 (2004).

Supplemental Material for “Memory Effects in Quantum State Verification”

The contents of the supplementary material are structured as follows: In Appendix A, we articulate two optimization targets within the framework of two-copy verification, specifically substantiating Theorem 1. In Appendix B, we establish connections between optimal verification protocols and optimal information-preserving channels, essential for the development of a two-copy graph state verification protocol. In Appendix C, we prove the graph state disentangled equation presented in Theorem 6, a crucial component in constructing state-disentangled channels and applicable to tasks such as distributed quantum computation and fault-tolerant quantum computation. In Appendices D and E, we discuss the details concerning the optimal verification strategy for graph states and show that this strategy could be used in fidelity estimation. In Appendix F, we give an explicit construction of verification strategies based on the dimension expansion technique.

Appendix A: Two-copy verification strategy optimization

In this section, we simplified the optimization in Eq. (4) of the main text (MT) with $k = 2$ and prove the main Theorem 1.

1. Reduce to fake pure states

First of all, one can easily prove that it suffices to optimize over pure states.

Lemma 1. *The maximal passing probability $p(\Omega)$, defined in Eq. (4) of MT, can be achieved among pure states, i.e.,*

$$p(\Omega) = \max_{\substack{|\sigma\rangle, |\sigma'\rangle \\ |\langle\psi|\sigma\rangle|^2 \leq 1-\varepsilon \\ |\langle\psi|\sigma'\rangle|^2 \leq 1-\varepsilon}} \text{Tr}[\Omega(|\sigma\rangle\langle\sigma| \otimes |\sigma'\rangle\langle\sigma'|)]. \quad (\text{A1})$$

Proof. We noted that this proof will be correct even if the fake state is classical-correlated. Since the maximum condition only reach on the product states without classical correlation.

According to Eq. (4), we have

$$p(\Omega) = \max_{\substack{\sigma, \sigma' \\ \langle\psi|\sigma|\psi\rangle \leq 1-\varepsilon \\ \langle\psi|\sigma'|\psi\rangle \leq 1-\varepsilon}} \text{Tr}[\Omega(\sigma \otimes \sigma')]. \quad (\text{A2})$$

We prove by contradiction that Eq. (A2) can be optimized over pure states. Assume that two mixed states σ and σ' achieve Eq. (A2); i.e., $p(\Omega) = \text{Tr}[\Omega(\sigma \otimes \sigma')]$. Notice that the set of fake states $\mathcal{S} := \{\sigma \mid \langle\psi|\sigma|\psi\rangle \leq 1 - \varepsilon\}$ is a convex set. Subsequently, the set of pure states $\mathcal{P} := \{|\sigma\rangle \mid |\langle\psi|\sigma\rangle|^2 \leq 1 - \varepsilon\}$ contain the extreme points of the set \mathcal{S} . Given that both $\sigma, \sigma' \in \mathcal{S}$, it is always possible to identify two pure-state decompositions

$$\sigma = \sum_j \alpha_j |\sigma_j\rangle\langle\sigma_j|, \quad \sigma' = \sum_k \beta_k |\sigma'_k\rangle\langle\sigma'_k|, \quad (\text{A3})$$

such that $\sum_j \alpha_j = 1$, $\sum_k \beta_k = 1$, and $|\sigma_j\rangle, |\sigma'_k\rangle \in \mathcal{P}$ for all j and k , i.e., they are the extreme points within the set \mathcal{P} . Let j_* and k_* be the two indices whose corresponding pure states $|\sigma_{j_*}\rangle$ and $|\sigma'_{k_*}\rangle$ achieve the following maximization:

$$\text{Tr}[\Omega(|\sigma_{j_*}\rangle\langle\sigma_{j_*}| \otimes |\sigma'_{k_*}\rangle\langle\sigma'_{k_*}|)] = \max_{j,k} \text{Tr}[\Omega(|\sigma_j\rangle\langle\sigma_j| \otimes |\sigma'_k\rangle\langle\sigma'_k|)]. \quad (\text{A4})$$

Then the passing probability was evaluated to

$$p(\Omega) = \text{Tr}[\Omega(\sigma \otimes \sigma')] = \sum_{jk} \alpha_j \beta_k \text{Tr}[\Omega(|\sigma_j\rangle\langle\sigma_j| \otimes |\sigma'_k\rangle\langle\sigma'_k|)] \quad (\text{A5})$$

$$\leq \sum_{jk} \alpha_j \beta_k \text{Tr}[\Omega(|\sigma_{j_*}\rangle\langle\sigma_{j_*}| \otimes |\sigma'_{k_*}\rangle\langle\sigma'_{k_*}|)] \quad (\text{A6})$$

$$= \text{Tr}[\Omega(|\sigma_{j_*}\rangle\langle\sigma_{j_*}| \otimes |\sigma'_{k_*}\rangle\langle\sigma'_{k_*}|)]. \quad (\text{A7})$$

That is to say, we can always identify two pure states— $|\sigma_{j_*}\rangle, |\sigma'_{k_*}\rangle \in \mathcal{S}$ —that lead to a passing probability larger than $\text{Tr}[\Omega(\sigma \otimes \sigma')]$, leading to a contradiction. We are done. \square

Thanks to Lemma 1, we can restrain the fake state to the tensor product form of pure states as below:

$$|\sigma\rangle \otimes |\sigma'\rangle = \sqrt{(1-\varepsilon_r)(1-\varepsilon'_r)}|\psi\psi\rangle + \sqrt{(1-\varepsilon_r)\varepsilon'_r}|\psi\psi^\perp\rangle + \sqrt{\varepsilon_r(1-\varepsilon'_r)}|\psi^\perp\psi\rangle + \sqrt{\varepsilon_r\varepsilon'_r}|\psi^\perp\psi^\perp\rangle, \quad (\text{A8})$$

where $\varepsilon_r, \varepsilon'_r \geq \varepsilon$ and $|\psi^\perp\rangle, |\psi'^\perp\rangle$ are pure states orthogonal to $|\psi\rangle$. Correspondingly, the passing probability evaluates to

$$\begin{aligned} \langle \sigma\sigma' | \Omega | \sigma\sigma' \rangle &= \sqrt{(1-\varepsilon_r)(1-\varepsilon'_r)(1-\varepsilon_r)(1-\varepsilon'_r)} \langle \psi\psi | \Omega | \psi\psi \rangle + \sqrt{(1-\varepsilon_r)(1-\varepsilon'_r)\varepsilon_r(1-\varepsilon'_r)} \langle \psi\psi | \Omega | \psi\psi^\perp \rangle \\ &\quad + \sqrt{(1-\varepsilon_r)(1-\varepsilon'_r)\varepsilon_r(1-\varepsilon'_r)} \langle \psi\psi | \Omega | \psi^\perp\psi \rangle + \sqrt{(1-\varepsilon_r)(1-\varepsilon'_r)\varepsilon_r\varepsilon'_r} \langle \psi\psi | \Omega | \psi^\perp\psi^\perp \rangle \\ &\quad + \sqrt{(1-\varepsilon_r)\varepsilon'_r(1-\varepsilon_r)(1-\varepsilon'_r)} \langle \psi\psi^\perp | \Omega | \psi\psi \rangle + \sqrt{(1-\varepsilon_r)\varepsilon'_r(1-\varepsilon_r)\varepsilon'_r} \langle \psi\psi^\perp | \Omega | \psi\psi^\perp \rangle \\ &\quad + \sqrt{(1-\varepsilon_r)\varepsilon'_r\varepsilon_r(1-\varepsilon'_r)} \langle \psi\psi^\perp | \Omega | \psi^\perp\psi \rangle + \sqrt{(1-\varepsilon_r)\varepsilon'_r\varepsilon_r\varepsilon'_r} \langle \psi\psi^\perp | \Omega | \psi^\perp\psi^\perp \rangle \\ &\quad + \sqrt{\varepsilon_r(1-\varepsilon'_r)(1-\varepsilon_r)(1-\varepsilon'_r)} \langle \psi^\perp\psi | \Omega | \psi\psi \rangle + \sqrt{\varepsilon_r(1-\varepsilon'_r)(1-\varepsilon_r)\varepsilon'_r} \langle \psi^\perp\psi | \Omega | \psi\psi^\perp \rangle \\ &\quad + \sqrt{\varepsilon_r(1-\varepsilon'_r)\varepsilon_r(1-\varepsilon'_r)} \langle \psi^\perp\psi | \Omega | \psi^\perp\psi \rangle + \sqrt{\varepsilon_r(1-\varepsilon'_r)\varepsilon_r\varepsilon'_r} \langle \psi^\perp\psi | \Omega | \psi^\perp\psi^\perp \rangle \\ &\quad + \sqrt{\varepsilon_r\varepsilon'_r(1-\varepsilon_r)(1-\varepsilon'_r)} \langle \psi^\perp\psi^\perp | \Omega | \psi\psi \rangle + \sqrt{\varepsilon_r\varepsilon'_r(1-\varepsilon_r)\varepsilon'_r} \langle \psi^\perp\psi^\perp | \Omega | \psi\psi^\perp \rangle \\ &\quad + \sqrt{\varepsilon_r\varepsilon'_r\varepsilon_r(1-\varepsilon'_r)} \langle \psi^\perp\psi^\perp | \Omega | \psi^\perp\psi \rangle + \sqrt{\varepsilon_r\varepsilon'_r\varepsilon_r\varepsilon'_r} \langle \psi^\perp\psi^\perp | \Omega | \psi^\perp\psi^\perp \rangle \\ &=: p(\Omega, \varepsilon_r, \varepsilon'_r, \psi, \psi'). \end{aligned} \quad (\text{A9})$$

$$(\text{A10})$$

Any reasonable two-copy verification strategy Ω must satisfy the following two conditions:

$$\Omega|\psi\rangle \otimes |\psi\rangle = |\psi\rangle \otimes |\psi\rangle, \quad (\text{A11})$$

$$\Omega = \mathbb{F}_{1\leftrightarrow 2} \Omega \mathbb{F}_{1\leftrightarrow 2}. \quad (\text{A12})$$

The first property is justifiable because, for any Ω failing to meet this condition, the inequality $N_m(\Omega) \geq 2p(1-p)1/\varepsilon^2 \ln 1/\delta$ is valid when ε is sufficiently small [31]. Here, $p = \text{Tr}[\Omega(|\psi\rangle\langle\psi| \otimes |\psi\rangle\langle\psi|)] \neq 1$. The quadratic nature of ε^2 leads to a considerably higher sampling complexity compared to those satisfying the first condition when ε is small. The second condition is rationalized by the fact that the verifier can employ classical randomness to execute the LOCC strategy $\frac{1}{2}(\Omega + \mathbb{F}_{1\leftrightarrow 2} \Omega \mathbb{F}_{1\leftrightarrow 2})$ based on any existing LOCC strategy Ω that might not fulfill the second condition.

2. Discussion on the insurance infidelity

In this section, we exclusively discuss the existence condition and upper bound of the insurance infidelity ε_{\max} .

Proposition 2. *Let $|\psi\rangle$ represent the target state and Ω denote its two-copy verification strategy, which exhibits symmetry under copy exchange. We define $\gamma_*(\Omega)$ and $\xi_*(\Omega)$ as the maximum eigenvalues of the operators $\mathbb{P}_\psi \mathbb{F}_{1\leftrightarrow 2} \Omega \mathbb{P}_\psi$ and $\mathbb{P}_\psi (\mathbb{F}_{1\leftrightarrow 2}/2 + \mathbb{I}_{12}) \Omega \mathbb{P}_\psi$, respectively, where $\mathbb{F}_{1\leftrightarrow 2}$ and \mathbb{P}_ψ are defined in Eq. (6) of MT. When ε is sufficiently small ($\varepsilon \ll 1$) and it is guaranteed that $\xi_*(\Omega) + \gamma_*(\Omega)/2 < 1$, for any choice of $|\psi^\perp\rangle$ and $|\psi'^\perp\rangle$, the function:*

$$p(\varepsilon'_r, \varepsilon_r, |\psi^\perp\rangle, |\psi'^\perp\rangle) = \langle \sigma\sigma' | \Omega | \sigma\sigma' \rangle, \quad (\text{A13})$$

reaches its maximum at the point $(\varepsilon_r, \varepsilon'_r) = (\varepsilon, \varepsilon)$ within a local region $R = \{(\varepsilon_r, \varepsilon'_r) | \varepsilon_r, \varepsilon'_r > \varepsilon, \varepsilon_r + \varepsilon'_r < 2\varepsilon_{\max}\}$. Additionally, ε_{\max} , referred to as the insurance infidelity, is unrelated to $|\psi^\perp\rangle$ and $|\psi'^\perp\rangle$, and must satisfy either of the following conditions:

1. If $\sqrt{\varepsilon} \ll \gamma_*(\Omega)$, then $\varepsilon_{\max} = 0.5\varepsilon + 0.5\varepsilon [(1 - \xi_*(\Omega) + 0.5\gamma_*(\Omega)) / \gamma_*(\Omega)]^2 > \varepsilon$.
2. If $\sqrt{\varepsilon} \sim \gamma_*(\Omega)$, then $\varepsilon_{\max} \gg \varepsilon$.

Proof. Given the sufficiently small nature of ε , we initially approximate ε_r and ε'_r as approximately equal to ε , resulting in the simplified expression for the passing probability:

$$p = 1 - \varepsilon_r - \varepsilon'_r + \langle \psi\psi^\perp | \Omega | \psi\psi^\perp \rangle \varepsilon_r + \langle \psi\psi^\perp | \Omega | \psi\psi^\perp \rangle \varepsilon'_r + (\langle \psi^\perp\psi | \Omega | \psi\psi^\perp \rangle + \langle \psi^\perp\psi | \Omega | \psi\psi^\perp \rangle) \sqrt{\varepsilon_r\varepsilon'_r} + \mathcal{O}(\varepsilon^{1.5}). \quad (\text{A14})$$

The leading orders dominate the behavior of the function p in the vicinity of the $(\varepsilon, \varepsilon)$ region. Therefore, our task is to demonstrate that the leading term reaches a local maximum at the point $(\varepsilon, \varepsilon)$ under the constraint $\varepsilon_r, \varepsilon'_r > \varepsilon$. To facilitate this analysis, we introduce the variable transformation $(x, x') = (\sqrt{\varepsilon_r}, \sqrt{\varepsilon'_r})$, after which the leading term undergoes a transformation to:

$$p_{\text{lead}} = 1 - (1 - R)x^2 - (1 - R')x'^2 + (B + B')xx', \quad (\text{A15})$$

where $x, x' > \sqrt{\varepsilon}$ and

$$R = \langle \psi \psi^\perp | \Omega | \psi \psi^\perp \rangle, \quad R' = \langle \psi \psi'^\perp | \Omega | \psi \psi'^\perp \rangle, \quad (\text{A16})$$

$$B = \langle \psi^\perp \psi | \Omega | \psi \psi^\perp \rangle, \quad B' = \langle \psi'^\perp \psi | \Omega | \psi \psi'^\perp \rangle. \quad (\text{A17})$$

We first noticed that:

$$\frac{\partial p_{\text{lead}}}{\partial x} = -2(1 - R)x + (B + B')x', \quad (\text{A18})$$

$$\frac{\partial p_{\text{lead}}}{\partial x'} = -2(1 - R')x' + (B + B')x. \quad (\text{A19})$$

To achieve a local maximum at $(\sqrt{\varepsilon}, \sqrt{\varepsilon})$ under the constraint $x, x' > \sqrt{\varepsilon}$, both derivatives at the point $x = x' = \sqrt{\varepsilon}$ must be less than zero for arbitrary $|\psi^\perp\rangle$ and $|\psi'^\perp\rangle$. This implies that:

$$\forall |\psi^\perp\rangle, |\psi'^\perp\rangle, \quad 1 > \frac{B}{2} + R + \frac{B'}{2}, \quad 1 > \frac{B}{2} + R' + \frac{B'}{2}. \quad (\text{A20})$$

Subsequently, we establish two critical values for the operator Ω with respect to the quantum state $|\psi\rangle$

$$\gamma_*(\Omega) = \max_{|\psi^\perp\rangle} \langle \psi^\perp \psi | \Omega | \psi \psi^\perp \rangle, \quad (\text{A21})$$

$$\xi_*(\Omega) = \max_{|\psi^\perp\rangle} \left(\frac{1}{2} \langle \psi^\perp \psi | \Omega | \psi \psi^\perp \rangle + \langle \psi \psi^\perp | \Omega | \psi \psi^\perp \rangle \right). \quad (\text{A22})$$

Utilizing these values, the local maximum condition is equivalent to the assertion that:

$$1 > \max_{|\psi^\perp\rangle} \left(\frac{1}{2} \langle \psi^\perp \psi | \Omega | \psi \psi^\perp \rangle + \langle \psi \psi^\perp | \Omega | \psi \psi^\perp \rangle \right) + \frac{1}{2} \max_{|\psi'^\perp\rangle} \left(\langle \psi'^\perp \psi | \Omega | \psi \psi'^\perp \rangle \right) \quad (\text{A23})$$

$$= \xi_*(\Omega) + \frac{1}{2} \gamma_*(\Omega). \quad (\text{A24})$$

In order to delineate the range of this local maximum, we initially assume that $\gamma_*(\Omega) \gg \sqrt{\varepsilon}$. Subsequently, we designate the selections of ψ^\perp and ψ'^\perp and find the domain where the p_{lead} always decreases as both variables x and x' increased. This region is delimited by two linear constraints:

$$\frac{\partial p_{\text{lead}}}{\partial x} = -2(1 - R)x + (B + B')x' < 0, \quad \frac{\partial p_{\text{lead}}}{\partial x'} = -2(1 - R)x' + (B + B')x < 0. \quad (\text{A25})$$

The local maximum condition ensures that $2(1 - R) > B + B'$. Consequently, every point within the set $R(R, B, B') = \{(x, x') | x, x' > \sqrt{\varepsilon}, x^2 + x'^2 < d(R, B, B')\}$ should decrease as both (x, x') increase, as depicted in Figure 5. Here, $d(R, B, B')$ is defined as follows:

$$d(R, B, B') = \varepsilon + \varepsilon \left(1 + 2 \frac{1 - (R + \frac{B}{2}) - \frac{B'}{2}}{B + B'} \right)^2 \quad (\text{A26})$$

$$> \varepsilon + \varepsilon \left(1 + 2 \frac{1 - \max_{|\psi^\perp\rangle} (R + \frac{B}{2}) - \max_{|\psi'^\perp\rangle} \frac{B'}{2}}{\max_{|\psi^\perp\rangle} B + \max_{|\psi'^\perp\rangle} B'} \right)^2 \quad (\text{A27})$$

$$= \varepsilon + \varepsilon \left(1 + \frac{1 - \xi_*(\Omega) - \frac{1}{2} \gamma_*(\Omega)}{\gamma_*(\Omega)} \right)^2 \quad (\text{A28})$$

$$= \varepsilon + \varepsilon \left(\frac{1 - \xi_*(\Omega) + \frac{1}{2} \gamma_*(\Omega)}{\gamma_*(\Omega)} \right)^2. \quad (\text{A29})$$

Hence, within the region $R(R, B, B')$, the function p attains its maximum at the point $(x, x') = (\sqrt{\varepsilon}, \sqrt{\varepsilon})$. Given an arbitrary selection of ψ^\perp and ψ'^\perp , their intersection is determined as follows:

$$R = \bigcap_{\forall \psi^\perp, \psi'^\perp} R(R, B, B') \quad (\text{A30})$$

$$= \{(x, x') | x, x' > \sqrt{\varepsilon}, x^2 + x'^2 < \min_{\psi^\perp, \psi'^\perp} d(R, B, B')\} \quad (\text{A31})$$

$$= \{(\varepsilon_r, \varepsilon'_r) | \varepsilon_r, \varepsilon'_r > \varepsilon, \varepsilon_r + \varepsilon'_r < 2\varepsilon_{\text{max}}\}. \quad (\text{A32})$$

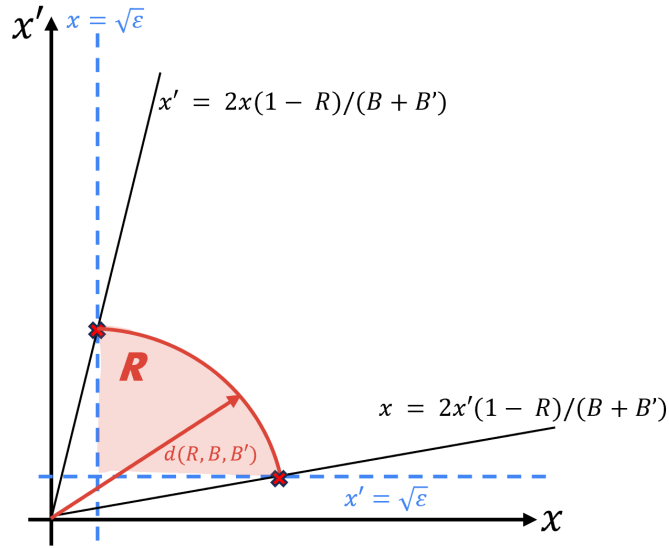


FIG. 5. This figure show the region R inside which p_{lead} reach local maximum at point $(\sqrt{\varepsilon}, \sqrt{\varepsilon})$. The insurance infidelity the could be calculated from the intersection of line $x' = 2x(1 - R)/(B + B')$ and $x = \sqrt{\varepsilon}$.

Here, $\varepsilon_{\max} = \min_{\psi^\perp, \psi'^\perp} d(R, B, B')/2$. The upper bound of d in Eq. (A29) provides the upper limit for ε_{\max}

$$\varepsilon_{\max} > \frac{1}{2}\varepsilon + \frac{1}{2}\varepsilon \left(\frac{1 - \xi_*(\Omega) + \frac{1}{2}\gamma_*(\Omega)}{\gamma_*(\Omega)} \right)^2 > \varepsilon. \quad (\text{A33})$$

In the last inequality, we invoke the local maximum condition once more, expressed as $1 > \xi_*(\Omega) + \frac{1}{2}\gamma_*(\Omega)$.

For strategies that satisfy $\gamma_*(\Omega) \sim \sqrt{\varepsilon}$, this upper bound is not valid. Other terms in the function p , such as $\langle \psi_m^\perp \psi_m^\perp | \Omega | \psi_m^\perp \psi_m^\perp \rangle$, must be considered. However, in this case, one can demonstrate that $|\varepsilon_{\max} - \varepsilon| \gg \varepsilon$ by recalculating the leading terms near ε :

$$p = 1 - \varepsilon_r - \varepsilon'_r + \langle \psi \psi^\perp | \Omega | \psi \psi^\perp \rangle \varepsilon_r + \langle \psi \psi'^\perp | \Omega | \psi \psi'^\perp \rangle \varepsilon'_r + \mathcal{O}(\varepsilon^{1.5}). \quad (\text{A34})$$

Given the projective construction, we have $\langle \psi \psi'^\perp | \Omega | \psi \psi'^\perp \rangle \leq 1$. Consequently, $(\varepsilon, \varepsilon)$ is the maximum in the region satisfying $|\varepsilon_r - \varepsilon| \sim \varepsilon$. This implies that $|\varepsilon_{\max} - \varepsilon| \gg \varepsilon$.

We can further simplify the expression of $\gamma_*(\Omega)$:

$$\gamma_*(\Omega) = \max_{|\psi^\perp\rangle} \langle \psi \psi^\perp | \mathbb{F}_{1 \leftrightarrow 2} \Omega | \psi \psi^\perp \rangle = \max_{|\Phi\rangle} \langle \Phi | \mathbb{P}_\psi \mathbb{F}_{1 \leftrightarrow 2} \Omega \mathbb{P}_\psi | \Phi \rangle, \quad (\text{A35})$$

where $\mathbb{P}_\psi = |\psi\rangle\langle\psi| \otimes (\mathbb{I} - |\psi\rangle\langle\psi|)$. Then, $\gamma_*(\Omega)$ is the maximum eigenvalue of the operator $\mathbb{P}_\psi \mathbb{F}_{1 \leftrightarrow 2} \Omega \mathbb{P}_\psi$. Similarly, $\xi_*(\Omega)$ corresponds to the maximum eigenvalue of operator $\mathbb{P}_\psi (\mathbb{F}_{1 \leftrightarrow 2} / 2 + \mathbb{I}_{12}) \Omega \mathbb{P}_\psi$. \square

3. Proof of Theorem 1 in MT

Now we prove Theorem 1 in MT.

Theorem 3 (Refined version of Theorem 1 in the main text). *Let Ω be an arbitrary two-copy verification strategy which is symmetric under copy exchange, we define $\lambda_*(\Omega)$ as the maximum eigenvalue of the operator $\Omega_* := 2\mathbb{P}_\psi \mathbb{P}_s \Omega \mathbb{P}_s \mathbb{P}_\psi$, where \mathbb{P}_s and \mathbb{P}_ψ are defined in Eq. (6) of MT. When ε is sufficiently small ($\varepsilon \ll 1$) and the local maximum condition in Proposition 2 is satisfied with insurance infidelity ε_{\max} . Then*

$$p(\Omega) = \max_{\substack{|\psi^\perp\rangle, |\psi'^\perp\rangle \\ \varepsilon_r, \varepsilon'_r \in [\varepsilon, \varepsilon_{\max}]}} \langle \sigma \sigma' | \Omega | \sigma \sigma' \rangle = 1 - 2(1 - \lambda_*(\Omega))\varepsilon + \mathcal{O}(\varepsilon^{1.5}), \quad (\text{A36})$$

Proof. We establish an additional critical maximum value for the operator Ω and the quantum state $|\psi\rangle$:

$$\lambda_*(\Omega) = \max_{|\psi^\perp\rangle} (\langle \psi\psi^\perp | \Omega | \psi\psi^\perp \rangle + \langle \psi^\perp\psi | \Omega | \psi^\perp\psi \rangle). \quad (\text{A37})$$

According to Proposition 2, the existence of insurance infidelity guarantees that $\xi_*(\Omega) + \frac{1}{2}\gamma_*(\Omega) < 1$. Consequently, $\lambda_*(\Omega) \leq \xi_*(\Omega) + \frac{\gamma_*(\Omega)}{2} < 1$.

Given the insurance infidelity ε_{\max} and the set R defined in Proposition 2, we observe that the set $S = \{(\varepsilon_r, \varepsilon'_r) | \varepsilon_r, \varepsilon'_r \in [\varepsilon, \varepsilon_{\max}]\}$ satisfies $S \subset R$. Therefore, $p(\Omega)$, being the maximum value within the region S with respect to variables $\psi^\perp, \psi'^\perp, \varepsilon_r$, and ε'_r , is attained solely at the constraint $(\varepsilon_r, \varepsilon'_r) = (\varepsilon, \varepsilon)$.

Further optimization over ψ and ψ^\perp is as follows:

$$p_{\max} = 1 - \max_{|\psi^\perp\rangle, |\psi'^\perp\rangle} [(1 - R - B) + (1 - R' - B')]\varepsilon + \mathcal{O}(\varepsilon^{1.5}) \quad (\text{A38})$$

$$= 1 - 2(1 - \lambda_*(\Omega))\varepsilon + \mathcal{O}(\varepsilon^{1.5}). \quad (\text{A39})$$

Again, given that $[\Omega, \mathbb{F}_{1\leftrightarrow 2}] = 0$, we can further simplify the expression of $\lambda_*(\Omega)$:

$$\lambda_*(\Omega) = \max_{|\psi^\perp\rangle} \langle \psi\psi^\perp | (\mathbb{F}_{1\leftrightarrow 2} + \mathbb{I}_{12})\Omega | \psi\psi^\perp \rangle \quad (\text{A40})$$

$$= \max_{|\Phi\rangle} \langle \Phi | \mathbb{P}_\psi (\mathbb{F}_{1\leftrightarrow 2} + \mathbb{I}_{12}) \Omega \mathbb{P}_\psi | \Phi \rangle \quad (\text{A41})$$

$$= \max_{|\Phi\rangle} \langle \Phi | 2\mathbb{P}_\psi \mathbb{P}_s \Omega \mathbb{P}_s \mathbb{P}_\psi | \Phi \rangle, \quad (\text{A42})$$

where

$$\mathbb{P}_\psi = |\psi\rangle\langle\psi| \otimes (\mathbb{I} - |\psi\rangle\langle\psi|), \quad \mathbb{P}_s = \frac{1}{2}(\mathbb{F}_{1\leftrightarrow 2} + \mathbb{I}_{12}). \quad (\text{A43})$$

Then, $\lambda_*(\Omega)$ is the maximum eigenvalue of the operator $\Omega_* = 2\mathbb{P}_\psi \mathbb{P}_s \Omega \mathbb{P}_s \mathbb{P}_\psi$. \square

4. Demonstrative example: The simple tensor product case

From Theorem 3, we know that to verify an arbitrary target state $|\psi\rangle$, we need to achieve the following objectives: (a) Construct families of local projective measurements that unconditionally accept $|\psi\rangle \otimes |\psi\rangle$ with certainty and exist insurance infidelity ε_{\max} , where Ω is the corresponding strategy; (b) Minimize $\lambda_*(\Omega)$ while maintaining ε_{\max} at a suitable value.

To benchmark the optimization tasks described above, we consider the strategy $\Omega = \Omega_l \otimes \Omega_l$, which is simply a tensor product of two single-copy strategies Ω_l . The operator Ω_* can be calculated as below:

$$\Omega_* = \frac{1}{2}\mathbb{P}_\psi (\mathbb{F}_{1\leftrightarrow 2} + \mathbb{I}_{12}) \Omega_l \otimes \Omega_l (\mathbb{F}_{1\leftrightarrow 2} + \mathbb{I}_{12}) \mathbb{P}_\psi \quad (\text{A44})$$

$$= \mathbb{P}_\psi \Omega_l \otimes \Omega_l \mathbb{P}_\psi + \mathbb{P}_\psi \frac{\mathbb{F}_{1\leftrightarrow 2} \Omega_l \otimes \Omega_l + \Omega_l \otimes \Omega_l \mathbb{F}_{1\leftrightarrow 2}}{2} \mathbb{P}_\psi \quad (\text{A45})$$

$$= \mathbb{P}_\psi \Omega_l \otimes \Omega_l \mathbb{P}_\psi \quad (\text{A46})$$

$$= |\psi\rangle\langle\psi| \otimes [(\mathbb{I} - |\psi\rangle\langle\psi|)\Omega_l (\mathbb{I} - |\psi\rangle\langle\psi|)], \quad (\text{A47})$$

where in the third equality we use the fact that $\mathbb{P}_\psi \mathbb{F}_{1\leftrightarrow 2} \Omega_l \otimes \Omega_l \mathbb{P}_\psi = 0$. Then $\lambda_*(\Omega) = \lambda_2(\Omega_l)$. This reduces to the standard single-copy verification efficiency as expected. Calculations also show that $\gamma_*(\Omega_l \otimes \Omega_l) = 0$, indicating that $\varepsilon_{\max} \gg \varepsilon$. In the following appendix, we construct a non-trivial two-copy strategy Ω for graph states, which satisfies that $\lambda_*(\Omega) = 0$, $\gamma_*(\Omega) = 0$, and $\varepsilon_{\max} > 1 - \varepsilon$.

Appendix B: Verification and information-preserving channel

To construct the two-copy verification strategy, we consider the case where the verifiers first implement the local operation and classical communication (LOCC) channel Λ . This channel treats the second copies as if they were an ideal graph state and utilizes this entanglement resource to implement a series of non-local gates to the first copy. These gates are designed to perform unitary rotations, transforming an identical graph state into the specific state $|0 \cdots 0\rangle$. Following this channel, everyone measures their first copies on the computational basis $\{|0\rangle\langle 0|, |1\rangle\langle 1|\}$ and passed the test if the results are all 0. For simplicity, we use

$|0\rangle_n = |0 \cdots 0\rangle$ to denote the basis state of n -qubits. For the expected state $|G\rangle \otimes |G\rangle$, it holds $\Lambda(|G\rangle\langle G| \otimes |G\rangle\langle G|) = |0\rangle\langle 0|_n \otimes |0\rangle\langle 0|_n$. To assess the efficiency for fake states, In this Appendix, we reformulate the optimization tasks in terms of information-preserving channels and establish the relation between channels and measurement operators as $\Omega_g = \Lambda^\dagger(|0\rangle\langle 0|_n \otimes |0\rangle\langle 0|_n)$. We need the following lemma, which follows directly from [32, Theorem 2].

Lemma 2. *Any LOCC measurement strategy can be decomposed and consequently implemented through a LOCC channel within the same Hilbert space, followed by a measurement in the computational basis with a specific selection of binomial measurement results that yield the “pass” outcome.*

One could set arbitrary binary string to the binomial measurement results with a “pass” outcome. However, the following theorem states that for a specific choice, $\{0 \cdots 0\}$, this strategy could formulate all the semi-optimal one-way strategies [12].

Theorem 4. *Any semi-optimal one-way strategy [12] can be constructed as a one-way LOCC channel followed by a binomial passing choice represented as $0 \cdots 0$.*

Proof. For a semi-optimal one-way strategy with target state $|\psi\rangle$, Alice chooses a measurement $|v_i\rangle\langle v_i|$ with results $i = 0, \dots, n$. Subsequently, Bob performs measurements on $|u_{t|i}\rangle\langle u_{t|i}|$ where $|u_{0|i}\rangle = \langle v_i|\psi\rangle$. In accordance with this, we define a unitary matrix U_i such that $|0\rangle = U_i|u_{0|i}\rangle$. The one-way LOCC channel can be expressed as

$$\Lambda(\rho) = \sum_i M_i \rho M_i^\dagger, \quad (\text{B1})$$

$$M_i = |0\rangle\langle v_i| \otimes U_i. \quad (\text{B2})$$

Subsequently, if Alice and Bob apply this channel first and then both measure on $|0\rangle\langle 0|, |1\rangle\langle 1|$ with the pass results represented by $|00\rangle$, they will get the same passing probability for any fake state σ . \square

Thus we consider all the strategies that set the "pass" binomial measurement results as $\{0 \cdots 0\}$ and gives the channel optimization task below:

Theorem 5 (Channel optimization). *Fix the choice of "pass" binomial measurement results as $\{0 \cdots 0\}$. Let's assume that n independent parties share a state $|\psi\rangle$. A LOCC channel Λ is optimal for verification if and only if it satisfies the following condition:*

1. $\Lambda(|\psi\rangle\langle\psi|) = |0 \cdots 0\rangle\langle 0 \cdots 0|$.
2. Any other LOCC channel Λ' satisfied the first condition will cancel more information on the difference between σ and $|\psi\rangle$ compared to Λ . In other words,

$$\text{Tr}[|\psi\rangle\langle\psi|\sigma] \leq \text{Tr}[\Lambda(|\psi\rangle\langle\psi|)\Lambda(\sigma)] \quad (\text{B3})$$

$$\leq \text{Tr}[\Lambda'(|\psi\rangle\langle\psi|)\Lambda'(\sigma)]. \quad (\text{B4})$$

This information-preserving channel, along with the verification strategy $\{\Omega, \mathbb{I} - \Omega\}$ constructed by this channel, then satisfies:

1. $\Omega = \Lambda^\dagger(|0 \cdots 0\rangle\langle 0 \cdots 0|)$.
2. $M_i|\psi\rangle = c_i|0 \cdots 0\rangle$. Here M_i is the Kraus operator of channel Λ , c_i is a constant parameter.
3. $\Lambda^\dagger(|0 \cdots 0\rangle\langle 0 \cdots 0|)|\psi\rangle = \sum_i c_i M_i^\dagger|0 \cdots 0\rangle = |\psi\rangle$.

Proof. We consider the strategy in which verifiers manipulate channel Λ first and pass with all qubits in the result $|0 \cdots 0\rangle\langle 0 \cdots 0|$. For any fake state σ , the passing probability is expressed as:

$$p(\Lambda) = \langle 0 \cdots 0|\Lambda(\sigma)|0 \cdots 0\rangle \quad (\text{B5})$$

$$= \text{Tr}[\Lambda(\sigma)\Lambda(|\psi \cdots \psi\rangle\langle\psi \cdots \psi|)] = \text{Tr}[\sigma\Lambda^\dagger(|0 \cdots 0\rangle\langle 0 \cdots 0|)]. \quad (\text{B6})$$

Consequently, we have derived the first conclusion that $\Omega = \Lambda^\dagger(|0 \cdots 0\rangle\langle 0 \cdots 0|)$. For any other channels, due to the second condition in the theorem, it must satisfy:

$$p(\Lambda') = \text{Tr}[\Lambda'(\sigma)\Lambda'(|\psi \cdots \psi\rangle\langle\psi \cdots \psi|)] \geq p(\Lambda). \quad (\text{B7})$$

A larger passing probability implies that the Ω' generated by Λ' will have less power to discern the fake state compared to Λ , showcasing the optimality of the channel construction within this fixed passing binomial choice. We suppose $M_i|\psi\rangle = c_i|\Phi_i\rangle$. Then the first condition becomes:

$$|c_i|^2 \sum_i |\Phi_i\rangle\langle\Phi_i| = |0\cdots 0\rangle\langle 0\cdots 0|. \quad (\text{B8})$$

Given that $|0\cdots 0\rangle\langle 0\cdots 0|$ is a pure state and lies at the boundary of the convex set, it implies that $|\Phi_i\rangle = |0\cdots 0\rangle$ must be satisfied, which proves the second conclusion. Regarding the last conclusion, we prove it with the calculations below:

$$\Lambda^\dagger(|0\cdots 0\rangle\langle 0\cdots 0|)|\psi\rangle = \sum_i M_i^\dagger |0\cdots 0\rangle\langle 0\cdots 0| M_i |\psi\rangle \quad (\text{B9})$$

$$= \sum_i c_i M_i^\dagger |0\cdots 0\rangle \quad (\text{B10})$$

$$= \sum_i M_i^\dagger M_i |\psi\rangle = |\psi\rangle. \quad (\text{B11})$$

In the last equality, we use the trace one condition on the channel where $\sum_i M_i^\dagger M_i = \mathbb{I}$. \square

1. Demonstrative example: Bell state

As a demonstrative example, we show that the single-copy optimal verification strategy for the Bell state [8] can be reformulated in terms of quantum channels. Specifically, the optimal strategy has the following form [8]

$$\Omega = \frac{1}{3}(P_{ZZ}^+ + P_{YY}^- + P_{XX}^+). \quad (\text{B12})$$

We construct the Karus operators according to this operator:

$$\Lambda(\rho) = \sum_{i=0}^5 M_i \rho M_i^\dagger, \quad (\text{B13})$$

$$M_0 = \frac{1}{\sqrt{3}}|0\rangle\langle 0| \otimes \mathbb{I}, \quad M_1 = \frac{1}{\sqrt{3}}|0\rangle\langle 1| \otimes X, \quad (\text{B14})$$

$$M_2 = \frac{1}{\sqrt{3}}|0\rangle\langle +| \otimes H, \quad M_3 = \frac{1}{\sqrt{3}}|0\rangle\langle -| \otimes XH, \quad (\text{B15})$$

$$M_4 = \frac{1}{\sqrt{3}}|0\rangle\langle +i| \otimes S^*, \quad M_5 = \frac{1}{\sqrt{3}}|0\rangle\langle -i| \otimes XS^*. \quad (\text{B16})$$

It is easy to check that $\sum_i M_i^\dagger M_i = \mathbb{I}$, $M_i|\Phi\rangle = |00\rangle/\sqrt{6}$, and

$$\Omega = \sum_{i=0}^5 M_i^\dagger |00\rangle\langle 00| M_i \equiv \Lambda^\dagger(|00\rangle\langle 00|). \quad (\text{B17})$$

We observe that

$$p = \text{Tr}[|00\rangle\langle 00| \Lambda(\sigma)] = \text{Tr}[\Lambda(|\psi\rangle\langle\psi|) \Lambda(\sigma)] \geq \text{Tr}[|\psi\rangle\langle\psi| \sigma]. \quad (\text{B18})$$

The inequality is satisfied if and only if Λ is a unitary channel. This represents the minimum passing probability for all measurement strategies and thus yields the globally optimal entangled measurement strategy $\{|\psi\rangle\langle\psi|, \mathbb{I} - |\psi\rangle\langle\psi|\}$, which may not always be realizable if only local operations and classical communication are allowed.

Appendix C: Non-local gates through graph state entanglement

In this Appendix, we show that graph states can function as an entanglement resource to locally implement non-local control- Z gates. In the following, we use CZ_{AB} and CX_{AB} to denote control- Z gate and control- X gate with control qubit A and target qubit B . We first prove the theorem below:

Theorem 6 (Graph state disentangled equation). *Through local interactions A_g between qubits O'_i in graph state $|G\rangle$ and auxiliary qubits O_i in state $|\omega\rangle$, the graph state $|G\rangle$ associated with graph $g = (V, E)$ can operate as an entanglement resource, yielding a non-local unitary transformation B_g on auxiliary qubits subject to local Pauli corrections denoted as $L_g(a)$ and $Q_g(a)$. Here a is a binary string that represents different measurement results of qubits O'_i on the computational basis. This non-local unitary matrix B_g can transform one identical graph state to $|0 \cdots 0\rangle$:*

$$A_g|\omega\rangle_O \otimes |G\rangle_{O'} = \frac{1}{\sqrt{2^{|V|}}} \sum_a L_g(a) B_g|\omega\rangle_O \otimes |a\rangle_{O'}, \quad (\text{C1})$$

where

$$A_g = \prod_{i \in V} H_{O_i} C_{O_i O'_i}, \quad (\text{C2})$$

$$L_g(a) = \prod_{(m,n) \in E} (-1)^{a_m a_n} X_{O_m}^{a_n} X_{O_n}^{a_m}, \quad (\text{C3})$$

$$B_g = \left(\prod_{i \in V} H_{O_i} \right) \times \left(\prod_{(m,n) \in E} CZ_{O_m O_n} \right). \quad (\text{C4})$$

Inversely, it holds that

$$A_g|G\rangle_O \otimes |\omega\rangle_{O'} = \frac{1}{\sqrt{2^{|V|}}} \sum_a L_g(a) Q_g(a) B_g|\omega\rangle_O \otimes |a\rangle_{O'}, \quad (\text{C5})$$

where

$$Q_g(a) = \prod_{i \in V} Z_{O_i}^{a_i}. \quad (\text{C6})$$

Proof. To prove Theorem 6, it suffices to demonstrate the correctness of two disentangled equations below.

$$\begin{aligned} & \langle a|_{O'} \left(\prod_{i \in V} H_{O_i} C_{O_i O'_i} \right) \times \left(\prod_{(m,n) \in E} CZ_{O'_m O'_n} \right) |+\rangle_{O'} \\ &= \frac{1}{\sqrt{2^{|V|}}} \left(\prod_{(m,n) \in E} (-1)^{a_m a_n} X_{O'_m}^{a_n} X_{O'_n}^{a_m} \right) \times \left(\prod_{i \in V} H_{O_i} \right) \times \left(\prod_{(m,n) \in E} CZ_{O_m O_n} \right), \end{aligned} \quad (\text{C7})$$

$$\begin{aligned} & \langle a|_{O'} \left(\prod_{i \in V} H_{O_i} C_{O_i O'_i} \right) \times \left(\prod_{(m,n) \in E} CZ_{O_m O_n} \right) |+\rangle_O \\ &= \frac{1}{\sqrt{2^{|V|}}} \left(\prod_{(m,n) \in E} (-1)^{a_m a_n} X_{O'_m}^{a_n} X_{O'_n}^{a_m} \right) \times \left(\prod_{i \in V} Z_{O_i}^{a_i} \right) \times \left(\prod_{i \in V} H_{O_i} \right) \times \left(\prod_{(m,n) \in E} CZ_{O_m O_n} \right) \mathbb{I}_{O'}. \end{aligned} \quad (\text{C8})$$

We decomposed the state $|\omega\rangle$ in the computational basis: $|\omega\rangle = \sum_p \lambda_p |p_0 \cdots p_N\rangle$. For Eq. (C7), we calculate the expression below:

$$2^{|V|} \text{LHS } |\omega\rangle_O = \sqrt{2^{|V|}} \sum_{p,q} \langle a|_{O'} \prod_{i \in V} H_{O_i} C_{O_i O'_i} \prod_{(m,n) \in E} (-1)^{q_m q_n} \lambda_p |p_0 \cdots p_N\rangle_O \otimes |q_0 \cdots q_N\rangle_{O'} \quad (\text{C9})$$

$$= \sum_{p,q,u} \lambda_p (-1)^{\sum_{i=0}^N u_i p_i} \prod_{(m,n) \in E} (-1)^{q_m q_n} \langle a|q_0 + p_0, \cdots, q_N + p_N\rangle |u_0, \cdots, u_N\rangle_O \quad (\text{C10})$$

$$= \sum_{p,u} \lambda_p (-1)^{\sum_{i=0}^N u_i p_i} \prod_{(m,n) \in E} (-1)^{(a_m + p_m)(a_n + p_n)} |u_0, \cdots, u_N\rangle_O \quad (\text{C11})$$

$$= \sum_{p,u} \lambda_p (-1)^{\sum_{i=0}^N u_i p_i} \prod_{(m,n) \in E} (-1)^{a_m \cdot a_n} \prod_{(m,n) \in E} (-1)^{p_m \cdot p_n} \prod_{(m,n) \in E} (-1)^{a_m \cdot p_n + p_m \cdot a_n} |u_0, \cdots, u_N\rangle_O. \quad (\text{C12})$$

$$2^{|V|} \text{RHS } |\omega\rangle_O = \sqrt{2^{|V|}} \sum_p \lambda_p \prod_{(m,n) \in E} (-1)^{a_m a_n} \left(\prod_{(m,n) \in E} X_{O_m}^{a_n} X_{O_n}^{a_m} \right) \left(\prod_{i \in V} H_{O_i} \right) \times \left(\prod_{(m,n) \in E} CZ_{O_m O_n} \right) |p_0 \cdots p_N\rangle_O \quad (\text{C13})$$

$$= \sum_{u,p} \lambda_p \prod_{(m,n) \in E} (-1)^{a_m a_n} \left(\prod_{(m,n) \in E} X_{O_m}^{a_n} X_{O_n}^{a_m} \right) (-1)^{\sum_{i=0}^N u_i p_i} \times \prod_{(m,n) \in E} (-1)^{p_m p_n} |u_0 \cdots u_N\rangle_O \quad (\text{C14})$$

$$= \sum_{u,p} \lambda_p (-1)^{\sum_{i=0}^N u_i p_i} \prod_{(m,n) \in E} (-1)^{a_m a_n} \prod_{(m,n) \in E} (-1)^{p_m p_n} \left(\prod_{(m,n) \in E} X_{O_m}^{a_n} X_{O_n}^{a_m} \right) |u_0 \cdots u_N\rangle_O \quad (\text{C15})$$

$$= \sum_{p,u'} \lambda_p (-1)^{\sum_{i=0}^N u'_i p_i} \prod_{(m,n) \in E} (-1)^{a_m \cdot a_n} \prod_{(m,n) \in E} (-1)^{p_m \cdot p_n} \prod_{(m,n) \in E} (-1)^{a_m \cdot p_n + p_m \cdot a_n} |u'_0, \dots, u'_N\rangle_O. \quad (\text{C16})$$

This coincidence proves Eq. (C7). For Eq. (C8), the same calculation proceeds as follows:

$$2^{|V|} \text{LHS } |\omega\rangle_{O'} = \sqrt{2^{|V|}} \sum_{p,q} \langle a' | \prod_{i \in V} H_{O_i} C_{O_i O'_i} \prod_{(m,n) \in E} (-1)^{q_m q_n} \lambda_p |q_0 \cdots q_N\rangle_O \otimes |p_0 \cdots p_N\rangle_{O'} \quad (\text{C17})$$

$$= \sum_{p,q,u} \lambda_p (-1)^{\sum_{i=0}^N u_i q_i} \prod_{(m,n) \in E} (-1)^{q_m q_n} \langle a | q_0 + p_0, \dots, q_N + p_N \rangle |u_0, \dots, u_N\rangle_O \quad (\text{C18})$$

$$= \sum_{p,u} \lambda_p (-1)^{\sum_{i=0}^N u_i (a_i + p_i)} \prod_{(m,n) \in E} (-1)^{(a_m + p_m)(a_n + p_n)} |u_0, \dots, u_N\rangle_O \quad (\text{C19})$$

$$= \sum_{p,u} \lambda_p (-1)^{\sum_{i=0}^N u_i p_i} \prod_{(m,n) \in E} (-1)^{a_m \cdot a_n} \prod_{(m,n) \in E} (-1)^{p_m \cdot p_n} (-1)^{\sum_{i=0}^N u_i a_i} \prod_{(m,n) \in E} (-1)^{a_m \cdot p_n + p_m \cdot a_n} |u_0, \dots, u_N\rangle_O. \quad (\text{C20})$$

$$2^{|V|} \text{RHS } |\omega\rangle_{O'} = \sum_{u,p} \lambda_p \prod_{(m,n) \in E} (-1)^{a_m a_n} \left(\prod_{(m,n) \in E} X_{O_m}^{a_n} X_{O_n}^{a_m} \right) (-1)^{\sum_{i=0}^N u_i a_i} (-1)^{\sum_{i=0}^N u_i p_i} \times \prod_{(m,n) \in E} (-1)^{p_m p_n} |u_0 \cdots u_N\rangle_O \quad (\text{C21})$$

$$= \sum_{u,p} \lambda_p (-1)^{\sum_{i=0}^N u_i p_i} \prod_{(m,n) \in E} (-1)^{a_m a_n} \prod_{(m,n) \in E} (-1)^{p_m p_n} (-1)^{\sum_{i=0}^N u_i a_i} \left(\prod_{(m,n) \in E} X_{O_m}^{a_n} X_{O_n}^{a_m} \right) |u_0 \cdots u_N\rangle_O \quad (\text{C22})$$

$$= \sum_{p,u'} \lambda_p (-1)^{\sum_{i=0}^N u'_i p_i} \prod_{(m,n) \in E} (-1)^{a_m \cdot a_n} \prod_{(m,n) \in E} (-1)^{p_m \cdot p_n} (-1)^{\sum_{i=0}^N u'_i a_i} \prod_{(m,n) \in E} (-1)^{a_m \cdot p_n + p_m \cdot a_n} |u'_0, \dots, u'_N\rangle_O. \quad (\text{C23})$$

This proves the Eq. (C8). \square

It is noteworthy that A_g represents local operations with respect to different verifiers because two-qubit gates $C_{O_i O'_i}$ can be locally realized in each verifier's quantum memory. However, the operator B_g in Theorem 6 involves non-local operations—Control-Z gates between qubits at different parties. This nonlocality arises from the consumption of the entanglement resource of the graph state $|G\rangle$.

Numerous pertinent observations merit discussion. Firstly, in the context of two qubits, the equation presented in Theorem 6 converges to the optimal local implementation of the CNOT gate, as elucidated in prior research [33]. Consequently, we anticipate that a singular entangled graph state, coupled with adjacent edge communication, will prove efficacious for the local implementation of control-Z gates between graph edges. This enables the restoration of a set of control-Z gates in the entangled state, which could be generated through Ising interactions, and facilitates rapid implementation of those gates on multiple remote computers via entanglement distribution and local gates. This methodology holds particular promise for applications in distributed quantum computation. Secondly, Theorem 6 proves to be instrumental in the domain of fault-tolerant computation, where transversal operations play a crucial role in mitigating fault propagation [34]. To illustrate this concept, consider the state $|\omega\rangle$ initialized with two computational bases, namely $|000\rangle$ and $|001\rangle$, with the ancillary graph state corresponding to stabilizers $XZZ, ZXZ, ZZ X$. Subsequently, the gate $B_g^\dagger = (\prod H_i) B_g (\prod H_i)$ encodes these two states into error correction codes with stabilizers XZZ, ZXZ , while A_g represents transversal operations involving Control-X gates and local Pauli gates. This transversal encoding strategy underscores its broad applicability to stabilizer states, given the inherent capacity of any stabilizer state to undergo transformation into a graph state through local Clifford (LC) operations [35]. Lastly, the presented theorem introduces an efficient two-copy verification strategy for graph states, as shown in the next section.

Appendix D: Two-copy verification for graph states

In the two-copy case, the optimization tasks can also be reframed from the channel perspective. For simplicity, we use $|\mathbf{0}\rangle$ to denote the vector $|0 \cdots 0\rangle$ in the first or second copy space. We consider the channel that regards $|\psi\rangle\langle\psi|$ as an entanglement resource to implement a nonlocal unitary transformation on the second copy, this unitary transformation rotates $|\psi\rangle$ to $|0 \cdots 0\rangle$ and $|\psi^\perp\rangle$ to another basis orthogonal to $|0 \cdots 0\rangle$. To formulate a $(n, d, 2)$ strategy for general graph states, we begin by constructing the Kraus operators, outlined below:

$$\Lambda(\rho) = \sum_{i=b_1 \cdots b_n} M_i \rho M_i^\dagger,$$

$$M_{b_1 \cdots b_n} = [L_g^\dagger(\mathbf{b}) \otimes |\mathbf{0}\rangle_n \langle \mathbf{b}|] \times A_g. \quad (\text{D1})$$

Consequently, the measurement operator takes the following form according to Theorem 5.

$$\Omega_g = \sum_{\mathbf{b}} A_g^\dagger [L_g(\mathbf{b}) |\mathbf{0}\rangle_n \langle \mathbf{0}| L_g^\dagger(\mathbf{b})] \otimes |\mathbf{b}\rangle \langle \mathbf{b}| A_g \quad (\text{D2})$$

$$= \sum_{b_1, \dots, b_n \in \{0,1\}} A_g^\dagger \bigotimes_{i=1}^n [\mathcal{P}(\sum_j b_j) \langle \mathcal{P}(\sum_j b_j) |_{O_i} \otimes |b_i\rangle \langle b_i|_{O'_i}] A_g \quad (\text{D3})$$

$(b_j, b_i) \in E \quad (b_j, b_i) \in E$

$$= \sum_{b_1, \dots, b_n \in \{0,1\}} A_g^\dagger \bigotimes_{i=0}^{N-1} [|c_i(\mathbf{b})\rangle \langle c_i(\mathbf{b})|_{O_i} \otimes |b_i\rangle \langle b_i|_{O'_i}] A_g. \quad (\text{D4})$$

Here, \mathcal{P} denotes a parity projection on 0 or 1, and $c_i(\mathbf{b})$ is a newly generated string according to string $\mathbf{b} = (b_1, \dots, b_n)$ and graph (V, E) . We term $c(\mathbf{b})$ the *graph parity string* of \mathbf{b} with respect to graph G , indicating that $c_i(\mathbf{b})$ at a specific vertex, i corresponds to the parity projection of the summation of all b_j at the adjacent vertices. It is worth noting that A_g^\dagger represents a basis transformation from the computational basis $|00\rangle, |01\rangle, |10\rangle, |11\rangle_{OO'}$ to four maximally entangled states:

$$|\Phi_{00}\rangle_{OO'} = \frac{|00\rangle + |11\rangle}{\sqrt{2}}, \quad |\Phi_{01}\rangle_{OO'} = \frac{|01\rangle + |10\rangle}{\sqrt{2}}, \quad |\Phi_{10}\rangle_{OO'} = \frac{|00\rangle - |11\rangle}{\sqrt{2}}, \quad |\Phi_{11}\rangle_{OO'} = \frac{|01\rangle - |10\rangle}{\sqrt{2}}. \quad (\text{D5})$$

The corresponding measurement operator is then given by:

$$\Omega_g = \sum_{\mathbf{b} \in \{0,1\}^n} \bigotimes_{j=1}^n |\Phi_{c_j(\mathbf{b})b_j}\rangle \langle \Phi_{c_j(\mathbf{b})b_j}|_{O_j O'_j}. \quad (\text{D6})$$

This operator indeed satisfy the symmetric condition of Eq. (A12) for the symmetric property of basis $|\Phi_{00}\rangle, |\Phi_{01}\rangle, |\Phi_{10}\rangle, |\Phi_{11}\rangle$ themselves. What's more, we can prove that Ω_g already attained the global-optimal lower bounds. To execute the strategy Ω_g , each party can measure their two qubits in the entanglement basis $|\Phi_{00}\rangle, |\Phi_{01}\rangle, |\Phi_{10}\rangle, |\Phi_{11}\rangle$ with corresponding measurement outcomes 00, 01, 10, 11. Subsequently, they separate their first and second digits to form the strings a and b , respectively, and verify whether b constitutes the graph parity string of a with respect to graph G .

If we define the state $|s_{inv}\rangle = |G\rangle \otimes |\omega\rangle$, applying Eq. (C5), we can deduce:

$$M_a |s_{inv}\rangle = \frac{1}{\sqrt{2^{|V|}}} (Q_g(a) \times B_g) \otimes \mathbb{I} |\omega\rangle \otimes |0 \cdots 0\rangle = \frac{1}{\sqrt{2^{|V|}}} V(a) \otimes \mathbb{I} |\omega\rangle \otimes |0 \cdots 0\rangle. \quad (\text{D7})$$

While the unitary operator $V(a)$ is associated with a , it consistently rotates the graph state into $|0 \cdots 0\rangle$ due to the stabilizing property of $Q(a)$ for the state $|0 \cdots 0\rangle$. In this case, we calculate that:

$$\Omega_g |s_{inv}\rangle = \Lambda^\dagger (|\mathbf{0}\rangle_n \langle \mathbf{0}| \otimes |\mathbf{0}\rangle_n \langle \mathbf{0}|) |s_{inv}\rangle = \sum_i M_i^\dagger |\mathbf{0}\rangle_n \langle \mathbf{0}| \otimes |\mathbf{0}\rangle_n \langle \mathbf{0}| M_i |s_{inv}\rangle \quad (\text{D8})$$

$$= \sum_i M_i^\dagger |\mathbf{0}\rangle_n \otimes |\mathbf{0}\rangle_n \times [\langle \mathbf{0}| \frac{1}{\sqrt{2^{|V|}}} V(a) |\omega\rangle] \quad (\text{D9})$$

$$= \langle G | \omega \rangle \sum_i \frac{1}{\sqrt{2^{|V|}}} M_i^\dagger |\mathbf{0}\rangle_n \otimes |\mathbf{0}\rangle_n \quad (\text{D10})$$

$$= \langle G | \omega \rangle \times |G\rangle \otimes |G\rangle. \quad (\text{D11})$$

The second equality relies on the fact that $V(a)$ unitarily transforms $|\psi\rangle$ to $|\mathbf{0}\rangle_n$. If we define the state $|s\rangle = |\omega\rangle \otimes |G\rangle$, where $|G\rangle$ is the graph state, employing Eq. (C1), it becomes evident that:

$$M_a|s\rangle = \frac{1}{\sqrt{2^{|V|}}} B_g|\omega\rangle \otimes |0 \cdots 0\rangle. \quad (\text{D12})$$

Here, B_g represents a unitary transformation that maps the graph state to $|0 \cdots 0\rangle$. Similarly

$$\Omega_g|s\rangle = \Lambda^\dagger(|\mathbf{0}\rangle\langle\mathbf{0}|_n \otimes |\mathbf{0}\rangle\langle\mathbf{0}|_n)|s\rangle = \sum_i M_i^\dagger |\mathbf{0}\rangle\langle\mathbf{0}|_n \otimes |\mathbf{0}\rangle\langle\mathbf{0}|_n M_i|s\rangle \quad (\text{D13})$$

$$= \sum_i M_i^\dagger |\mathbf{0}\rangle_n \otimes |\mathbf{0}\rangle_n \left[\langle\mathbf{0}| \frac{1}{\sqrt{2^{|V|}}} B_g|\omega\rangle \right] \quad (\text{D14})$$

$$= \langle G|\omega\rangle \sum_i \frac{1}{\sqrt{2^{|V|}}} M_i^\dagger |\mathbf{0}\rangle_n \otimes |\mathbf{0}\rangle_n \quad (\text{D15})$$

$$= \langle G|\omega\rangle |G\rangle \otimes |G'\rangle. \quad (\text{D16})$$

We refer to Λ as the self-disentangled channel of state $|\psi\rangle$. If we substitute $|\omega\rangle = |\psi\rangle = |G\rangle$, we will observe that Eq. (A11) is satisfied. If we substitute $|\omega\rangle = |\psi^\perp\rangle$, we see that:

$$\Omega_g \mathbb{P}_s |\psi\psi^\perp\rangle = \frac{1}{2} \Omega_g (|\psi\psi^\perp\rangle + |\psi^\perp\psi\rangle) = 0. \quad (\text{D17})$$

Now, we can calculate the operator Ω_\star in Theorem 3. First, we demonstrate that $\Omega_g \mathbb{P}_s \mathbb{P}_\psi = 0$:

$$\Omega_g \mathbb{P}_s \mathbb{P}_\psi = \Omega_g \sum_j \mathbb{P}_s |\psi\psi_j^\perp\rangle \langle\psi\psi_j^\perp| = \sum_j \langle\psi|\psi_j^\perp\rangle |\psi\psi\rangle \langle\psi\psi_j^\perp| = 0. \quad (\text{D18})$$

Then we conclude that $\Omega_\star = 2\mathbb{P}_\psi \mathbb{P}_s \Omega_g \mathbb{P}_s \mathbb{P}_\psi = 0$. Such a strategy corresponds to a scenario where $\lambda_\star(\Omega_g) = 0$. Similarly, we can show that $\Omega_g \mathbb{P}_\psi = 0$ and conclude that $\xi_\star(\Omega_g) = \gamma_\star(\Omega_g) = 0$. This means that $\varepsilon_{\max} \gg \varepsilon$. Thus, this implies that the verification efficiency is:

$$N_m(\Omega_g) = \frac{1}{\varepsilon(1 - \lambda_\star(\Omega_g)) + O(\varepsilon^{1.5})} \ln \frac{1}{\delta} = \frac{1}{\varepsilon + O(\varepsilon^{1.5})} \ln \frac{1}{\delta}. \quad (\text{D19})$$

When ε is sufficiently small, the efficiency converges to the globally optimal efficiency.

We can directly calculate the passing probability of strategy Ω_g as

$$p(\Omega_g) = \langle\sigma\sigma'|\Omega_g|\sigma\sigma'\rangle = (1 - \varepsilon_r)(1 - \varepsilon'_r) + \varepsilon_r \varepsilon'_r \langle\psi^\perp\psi'^\perp|\Omega_g|\psi^\perp\psi'^\perp\rangle \approx 1 - \varepsilon_r - \varepsilon'_r. \quad (\text{D20})$$

This equation also illustrates that Ω_g is already a global-optimal strategy itself. To evaluate ε_{\max} , we note that:

$$\frac{dp}{d\varepsilon_r} = -1 + \varepsilon'_r + \varepsilon'_r \langle\psi^\perp\psi'^\perp|\Omega_g|\psi^\perp\psi'^\perp\rangle, \quad (\text{D21})$$

$$\frac{dp}{d\varepsilon'_r} = -1 + \varepsilon_r + \varepsilon_r \langle\psi^\perp\psi'^\perp|\Omega_g|\psi^\perp\psi'^\perp\rangle. \quad (\text{D22})$$

Then the

$$\frac{dp}{d\varepsilon_r} - \frac{dp}{d\varepsilon'_r} = -(1 + \langle\psi^\perp\psi'^\perp|\Omega_g|\psi^\perp\psi'^\perp\rangle)(\varepsilon_r - \varepsilon'_r). \quad (\text{D23})$$

This implies that p reaches its maximum when $\varepsilon_r = \varepsilon'_r$. Subsequently, we simplify the function as follows:

$$p(\varepsilon_r) = 1 - 2\varepsilon_r + \varepsilon_r^2 [1 + \langle\psi^\perp\psi'^\perp|\Omega_g|\psi^\perp\psi'^\perp\rangle], \quad (\text{D24})$$

To confirm that this function reaches the maximum at $\varepsilon_r = \varepsilon$, we find another solution ε_{\max} such that $p(\varepsilon) = p(\varepsilon_{\max})$ is satisfied:

$$\varepsilon_{\max} = \frac{2}{1 + \langle\psi^\perp\psi'^\perp|\Omega_g|\psi^\perp\psi'^\perp\rangle} - \varepsilon > 1 - \varepsilon. \quad (\text{D25})$$

This provides a lower bound for ε_{\max} . For a sufficiently small ε , it is effective to verify that $\varepsilon_r > \varepsilon_{\max}$.

1. Demonstrative example: Two-copy Bell state verification

Here, we consider a straightforward scenario where two copies of the Bell states O_0, O_1 and O'_0, O'_1 are distributed to parties 0 and 1. A Bell state is equivalent to a graph state up to a unitary transformation $H_{O_0}H_{O'_0}$ applied to the Bell state. Thus, the Bell state can be efficiently verified by the two-copy verification operator, as illustrated in Table I:

$$\begin{aligned} \Omega_g = & |\Phi_{00}\rangle\langle\Phi_{00}|_{O_0O'_0} \otimes |\Phi_{00}\rangle\langle\Phi_{00}|_{O_1O'_1} + |\Phi_{11}\rangle\langle\Phi_{11}|_{O_0O'_0} \otimes |\Phi_{11}\rangle\langle\Phi_{11}|_{O_1O'_1} \\ & + |\Phi_{01}\rangle\langle\Phi_{01}|_{O_0O'_0} \otimes |\Phi_{10}\rangle\langle\Phi_{10}|_{O_1O'_1} + |\Phi_{10}\rangle\langle\Phi_{10}|_{O_0O'_0} \otimes |\Phi_{01}\rangle\langle\Phi_{01}|_{O_1O'_1}. \end{aligned} \quad (\text{D26})$$

Code (a_0, a_1)	Code (b_0, b_1)	Passing Measurement
(0, 0)	(0, 0)	$ \Phi_{00}\rangle\langle\Phi_{00} \otimes \Phi_{00}\rangle\langle\Phi_{00} $
(0, 1)	(1, 0)	$ \Phi_{10}\rangle\langle\Phi_{10} \otimes \Phi_{01}\rangle\langle\Phi_{01} $
(1, 0)	(0, 1)	$ \Phi_{01}\rangle\langle\Phi_{01} \otimes \Phi_{10}\rangle\langle\Phi_{10} $
(1, 1)	(1, 1)	$ \Phi_{11}\rangle\langle\Phi_{11} \otimes \Phi_{11}\rangle\langle\Phi_{11} $

TABLE I. The table presents all four graph parity codes for a two-qubit linear graph state. Each parity code corresponds to a projective measurement on the Bell basis. The weighted sum of these passing measurement operators lead to our strategy operator Ω_g .

Furthermore, we notice that

$$H_{O_0}H_{O'_0}|\Phi_{01}\rangle_{O_0O'_0} = |\Phi_{10}\rangle_{O_0O'_0}, \quad (\text{D27})$$

$$H_{O_0}H_{O'_0}|\Phi_{10}\rangle_{O_0O'_0} = |\Phi_{01}\rangle_{O_0O'_0}, \quad (\text{D28})$$

$$H_{O_0}H_{O'_0}|\Phi_{00}\rangle_{O_0O'_0} = |\Phi_{00}\rangle_{O_0O'_0}, \quad (\text{D29})$$

$$H_{O_0}H_{O'_0}|\Phi_{11}\rangle_{O_0O'_0} = |\Phi_{11}\rangle_{O_0O'_0}. \quad (\text{D30})$$

Therefore, the two-copy verification strategy of Bell state is given by:

$$\Omega_{\text{Bell}} = H_{O_0}H_{O'_0}\Omega_gH_{O_0}H_{O'_0} \quad (\text{D31})$$

$$\begin{aligned} = & |\Phi_{00}\rangle\langle\Phi_{00}|_{O_0O'_0} \otimes |\Phi_{00}\rangle\langle\Phi_{00}|_{O_1O'_1} + |\Phi_{11}\rangle\langle\Phi_{11}|_{O_0O'_0} \otimes |\Phi_{11}\rangle\langle\Phi_{11}|_{O_1O'_1} \\ & + |\Phi_{01}\rangle\langle\Phi_{01}|_{O_0O'_0} \otimes |\Phi_{01}\rangle\langle\Phi_{01}|_{O_1O'_1} + |\Phi_{10}\rangle\langle\Phi_{10}|_{O_0O'_0} \otimes |\Phi_{10}\rangle\langle\Phi_{10}|_{O_1O'_1}. \end{aligned} \quad (\text{D32})$$

It should be noted that this measurement operator in the 16×16 linear space may possess multiple unit eigenvalues. To numerically gauge its efficiency, we perform the Schmidt decomposition of the operator:

$$\begin{aligned} \Omega_{\text{Bell}} - |\psi\rangle\langle\psi| \otimes |\psi\rangle\langle\psi| &= \sum_i \Lambda_i M_{O_0, O_1}^{(i)} \otimes M_{O'_0, O'_1}^{(i)} \quad (\text{D33}) \\ &= \begin{pmatrix} 0.5 & 0 & 0 & -0.5 \\ 0 & 0 & 0 & 0 \\ 0 & 0 & 0 & 0 \\ -0.5 & 0 & 0 & 0.5 \end{pmatrix}_{O_0, O_1} \otimes \begin{pmatrix} 0.5 & 0 & 0 & -0.5 \\ 0 & 0 & 0 & 0 \\ 0 & 0 & 0 & 0 \\ -0.5 & 0 & 0 & 0.5 \end{pmatrix}_{O'_0, O'_1} \\ &\quad + \begin{pmatrix} 0 & 0 & 0 & 0 \\ 0 & 0 & \frac{1}{\sqrt{2}} & 0 \\ 0 & \frac{1}{\sqrt{2}} & 0 & 0 \\ 0 & 0 & 0 & 0 \end{pmatrix}_{O_0, O_1} \otimes \begin{pmatrix} 0 & 0 & 0 & 0 \\ 0 & 0 & \frac{1}{\sqrt{2}} & 0 \\ 0 & \frac{1}{\sqrt{2}} & 0 & 0 \\ 0 & 0 & 0 & 0 \end{pmatrix}_{O'_0, O'_1} \\ &\quad + \begin{pmatrix} 0 & 0 & 0 & 0 \\ 0 & \frac{1}{\sqrt{2}} & 0 & 0 \\ 0 & 0 & \frac{1}{\sqrt{2}} & 0 \\ 0 & 0 & 0 & 0 \end{pmatrix}_{O_0, O_1} \otimes \begin{pmatrix} 0 & 0 & 0 & 0 \\ 0 & \frac{1}{\sqrt{2}} & 0 & 0 \\ 0 & 0 & \frac{1}{\sqrt{2}} & 0 \\ 0 & 0 & 0 & 0 \end{pmatrix}_{O'_0, O'_1}. \end{aligned} \quad (\text{D34})$$

We observe that all three matrices satisfy $M^{(i)}|\psi\rangle = 0$. This indicates that the term $\Omega|\psi\rangle \otimes |\psi^\perp\rangle$ will vanish during the calculation. Now, let's consider the fake state $|\sigma\rangle \otimes |\sigma'\rangle$ according to Lemma 1 and calculate:

$$p(\Omega_{\text{Bell}}, |\sigma, \sigma'\rangle) = |\langle\psi|\sigma\rangle\langle\psi|\sigma'\rangle| + \langle\sigma\sigma'\rangle \left(\sum_i \Lambda_i M_{O_0, O_1}^{(i)} \otimes M_{O'_0, O'_1}^{(i)} \right) |\sigma\sigma'\rangle \quad (\text{D35})$$

$$= (1 - \varepsilon_r) \times (1 - \varepsilon'_r) + \varepsilon_r \varepsilon'_r \langle\psi^\perp\psi'^\perp| \left(\sum_i \Lambda_i M_{O_0, O_1}^{(i)} \otimes M_{O'_0, O'_1}^{(i)} \right) |\psi^\perp\psi'^\perp\rangle \quad (\text{D36})$$

$$\leq (1 - \varepsilon_r) \times (1 - \varepsilon'_r) + \varepsilon_r \varepsilon'_r. \quad (\text{D37})$$

When we only consider the fake state near the target state, where ε_r is sufficiently small, the linear term predominates. In this case, we can conclude that

$$p(\Omega_{\text{Bell}}, |\sigma, \sigma'\rangle) \leq (1 - \varepsilon_r) \times (1 - \varepsilon'_r) + \varepsilon_r \varepsilon'_r \leq (1 - \varepsilon)^2 + \varepsilon^2. \quad (\text{D38})$$

The condition that the fake state is near the target state is critical. Specifically, we observe that setting $\varepsilon_r = \varepsilon'_r = 1$ leads to $p(\Omega, |\sigma, \sigma'\rangle) = 1$, which is certainly greater than $(1 - \varepsilon)^2 + \varepsilon^2$. However, in this extreme case, the fake state $|\sigma\sigma'\rangle$ is already orthogonal to the target state $|\psi\rangle \otimes |\psi\rangle$. Therefore, this fake state can be easily verified with a standard single-copy strategy. After obtaining $p(\Omega_{\text{Bell}})$, we can draw conclusions according to Eq. (5):

$$N_m(\Omega_{\text{Bell}}) = \frac{2 \ln \delta}{\ln[(1 - 2\varepsilon + \varepsilon^2) + \varepsilon^2]}. \quad (\text{D39})$$

When both ε and δ are sufficiently small, the required number of copies scales as $1/\varepsilon \ln 1/\delta$, approaching the optimal strategy.

Appendix E: Fidelity estimation

For quantum devices that generate quantum states with independent and identical distribution, we can regard the fake state as two copies of $\sigma \otimes \sigma'$. Supposed that:

$$\sigma = \sum_i p_i |\sigma_i\rangle\langle\sigma_i|, \quad \sigma' = \sum_j p'_j |\sigma'_j\rangle\langle\sigma'_j|. \quad (\text{E1})$$

Here $|\sigma_i\rangle$ and $|\sigma'_j\rangle$ are both pure states that satisfy:

$$|\sigma_i\rangle = \sqrt{1 - \varepsilon_{ri}} |G\rangle + \sqrt{\varepsilon_{ri}} |G_i^\perp\rangle, \quad (\text{E2})$$

$$|\sigma'_j\rangle = \sqrt{1 - \varepsilon'_{rj}} |G\rangle + \sqrt{\varepsilon'_{rj}} |G_j'^\perp\rangle. \quad (\text{E3})$$

Then the fidelity of these two copies satisfied:

$$F := \langle G|\sigma|G\rangle = \sum_i p_i (1 - \varepsilon_{ri}), \quad F' := \langle G|\sigma'|G\rangle = \sum_j p'_j (1 - \varepsilon'_{rj}). \quad (\text{E4})$$

The passing rate of strategy Ω_g can be evaluated via

$$p_s = \text{Tr}[\Omega_g(\sigma \otimes \sigma')] = \sum_i \sum_j p_i p'_j \langle\sigma_i \sigma'_j | \Omega_g | \sigma_i \sigma'_j\rangle. \quad (\text{E5})$$

According to Eq. (D20),

$$\langle\sigma_i \sigma'_j | \Omega_g | \sigma_i \sigma'_j\rangle = (1 - \varepsilon_{ri})(1 - \varepsilon'_{rj}) + A_{ij} \varepsilon_{ri} \varepsilon'_{rj}, \quad (\text{E6})$$

where $A_{ij} := \langle G_i^\perp G_j'^\perp | \Omega_g | G_i^\perp G_j'^\perp\rangle$. Then p_s satisfies:

$$p_s = \sum_i \sum_j p_i p'_j [(1 - \varepsilon_{ri})(1 - \varepsilon'_{rj}) + A_{ij} \varepsilon_{ri} \varepsilon'_{rj}] \quad (\text{E7})$$

$$= \left[\sum_i p_i (1 - \varepsilon_{ri}) \right] \times \left[\sum_j p'_j (1 - \varepsilon'_{rj}) \right] + \sum_i \sum_j p_i p'_j A_{ij} \varepsilon_{ri} \varepsilon'_{rj} \quad (\text{E8})$$

$$= F \times F' + \sum_i \sum_j p_i p'_j A_{ij} \varepsilon_{ri} \varepsilon'_{rj}. \quad (\text{E9})$$

When the infidelity ε is sufficiently small, we have $(1 - F) \sim \mathcal{O}(\varepsilon)$ and $(1 - F') \sim \mathcal{O}(\varepsilon)$. Because $p_i, p'_j \in [0, 1]$, it holds that for all i and j ,

$$p_i \varepsilon_{ri} \sim \mathcal{O}(\varepsilon), \quad p'_j \varepsilon'_{rj} \sim \mathcal{O}(\varepsilon). \quad (\text{E10})$$

Thus, we can conclude that

$$p_s = \langle G|\sigma|G \rangle \cdot \langle G|\sigma'|G \rangle + \mathcal{O}(\varepsilon^2). \quad (\text{E11})$$

Appendix F: Illustrative example for dimension expansion strategy

In this section, we present the explicit dimension expansion construction of a $(2, 2, 2)$ -strategy applicable to the two-qubit state $|\psi_\theta\rangle = \cos\theta|00\rangle_{AB} + \sin\theta|11\rangle_{AB}$ distributed between two parties, denoted as A and B , representing a specific instance of GHZ-like states. A more generalized approach can be formulated similarly, drawing from the efficient $(n, 1, d)$ verification strategy proposed by Li *et al.* for GHZ-like qudit states [30]. According to the dimension expansion method outlined in the main text, this task is equivalent to identifying a $(2, 1, 2^2)$ strategy applicable to the GHZ-like qudit state of the form:

$$|\Psi_\theta\rangle := \cos^2\theta|\mathbf{0}\rangle_A \otimes |\mathbf{0}\rangle_B + \cos\theta \sin\theta(|\mathbf{1}\rangle_A \otimes |\mathbf{1}\rangle_B + |\mathbf{2}\rangle_A \otimes |\mathbf{2}\rangle_B) + \sin^2\theta|\mathbf{3}\rangle_A \otimes |\mathbf{3}\rangle_B. \quad (\text{F1})$$

This state corresponds to the 2-th tensor product state $|\psi_\theta\rangle^{\otimes 2}$ via the following identification: $|00\rangle \rightarrow |\mathbf{0}\rangle, |01\rangle \rightarrow |\mathbf{1}\rangle, |10\rangle \rightarrow |\mathbf{2}\rangle, |11\rangle \rightarrow |\mathbf{3}\rangle$.

In a previous study, various straightforward and efficient protocols were proposed for verifying bipartite qudit pure states such as $|\Psi_\theta\rangle$. Here, we employ a strategy based on a two-way LOCC (Local Operations and Classical Communication) strategy, denoted as Ω_{IV} in [30, Eq. (48)]. It is worth noting that alternative qudit measurement strategies offering higher efficiency can be chosen, leading to a different $(2, 2, 2)$ multi-copy strategy requiring fewer copies.

In the qudit verification strategy Ω_{IV} , five measurement bases are initially defined based on the five mutually unbiased bases (MUBs) for the four-dimensional space. Through the identification between qubit states and qudit states, these bases can be explicitly expressed as follows. It is important to note that the projective measurements onto the latter four sets of bases necessitate local interactions between two qubits in each party.

$$\begin{aligned} B_0 &: \{|00\rangle, |01\rangle, |10\rangle, |11\rangle\}, \\ B_1 &: \left\{ \frac{|00\rangle + |01\rangle + |10\rangle + |11\rangle}{2}, \frac{|00\rangle + |01\rangle - |10\rangle - |11\rangle}{2}, \frac{|00\rangle - |01\rangle - |10\rangle + |11\rangle}{2}, \frac{|00\rangle - |01\rangle + |10\rangle - |11\rangle}{2} \right\}, \\ B_2 &: \left\{ \frac{|00\rangle - |01\rangle - i|10\rangle - i|11\rangle}{2}, \frac{|00\rangle - |01\rangle + i|10\rangle + i|11\rangle}{2}, \frac{|00\rangle + |01\rangle + i|10\rangle - i|11\rangle}{2}, \frac{|00\rangle + |01\rangle - i|10\rangle + i|11\rangle}{2} \right\}, \\ B_3 &: \left\{ \frac{|00\rangle - i|01\rangle - i|10\rangle - |11\rangle}{2}, \frac{|00\rangle - i|01\rangle + i|10\rangle + |11\rangle}{2}, \frac{|00\rangle + i|01\rangle + i|10\rangle - |11\rangle}{2}, \frac{|00\rangle + i|01\rangle - i|10\rangle + |11\rangle}{2} \right\}, \\ B_4 &: \left\{ \frac{|00\rangle - i|01\rangle - |10\rangle - i|11\rangle}{2}, \frac{|00\rangle - i|01\rangle + |10\rangle + i|11\rangle}{2}, \frac{|00\rangle + i|01\rangle - |10\rangle + i|11\rangle}{2}, \frac{|00\rangle + i|01\rangle + |10\rangle - i|11\rangle}{2} \right\}. \end{aligned}$$

In the procedure of the $(2, 2, 2)$ multi-copy strategy derived from the qudit verification strategy Ω_{IV} , both parties have an equal probability of initiating a test. If the test commences with party A , it holds a probability p_0 of measuring its two qubits on the first MUBs B_0 . Additionally, party A possesses a probability of $(1 - p_0)/4$ for measurement on the remaining d^k mutually unbiased bases. Subsequently, party A communicates its measurement choice and results $|u_{li}\rangle$ to party B , where $|u_{li}\rangle$ denotes the i -th basis of the l -th set of MUBs. Party B then performs a measurement on the basis containing the reduced state $|v_{li}\rangle = \langle u_{li}|\Psi_\theta\rangle / |\langle u_{li}|\Psi_\theta\rangle|^2$ based on the message from Alice and passes the test if the result matches this reduced state.

Ref. [30] showed that setting $p_0 = (s_0^2 + s_1^2)/(2 + s_0^2 + s_1^2)$, where s_0 and s_1 represent the largest and second largest terms of the coefficient set $\{\cos^2\theta, \cos\theta \sin\theta, \sin^2\theta\}$, respectively, achieves the optimal strategy for verifying $|\Psi_\theta\rangle$. When $\theta \in (0, \pi/4)$, it holds that $s_0 = \cos^2\theta$ and $s_1 = \sin\theta \cos\theta$. Consequently, the second largest eigenvalues of the verification strategy for $|\Psi_\theta\rangle$ is given by $\lambda_2(\Omega_{\text{IV}}) = \cos^2\theta/(2 + \cos^2\theta)$. Utilizing the result from the main text, we can conclude that for small values of ε , the number of copies required to achieve a certain worst-case failure probability δ is upper bounded by

$$N_{\text{de},2}(\Omega_{\text{IV}}) = \frac{2 + \cos^2\theta}{2\varepsilon} \ln \frac{1}{\delta}. \quad (\text{F3})$$